Transport Economics and Management 3 (2025) 135–152

Contents lists available at ScienceDirect

Transport Economics and Management

journal homepage: www.journals.elsevier.com/transport-economics-and-management

Advanced Air Mobility for commuting? An exploration of economic, energy, and environmental feasibility

Daniel Perez [a], Heeseung Shon [a], Bo Zou [a,*], Kenneth Kuhn [b]

[a] Civil, Materials, and Environmental Engineering, University of Illinois Chicago, United States
[b] Walmart Global Tech, United States

ARTICLE INFO

Keywords:
Advanced Air Mobility (AAM)
Electric vertical takeoff and landing aircraft (eVTOL)
Commuting
Time-expanded network model
Economic feasibility
Energy and environmental feasibility

ABSTRACT

Advanced Air Mobility (AAM) presents an emerging alternative to traditional car driving for commuting in metropolitan areas. However, its feasibility has not been thoroughly studied nor well understood at the operational level. Given that AAM has not been in place, this study explores the economic, energy, and environmental feasibility of AAM for commuting at an early stage of AAM deployment. We propose a time-expanded network model to characterize the dynamics of eVTOL operations between a vertiport pair in different states: in-service flying, relocation flying, charging, and parking, while respecting various operational and commuter time window constraints. By jointly considering eVTOL flying with vertiport access and egress and using real-world data, we demonstrate an application of the model in the Chicago metropolitan area in the US. Different vertiport pairs and eVTOL aircraft models are investigated. We find substantial travel time saving if commuting by AAM. While vehicle operating cost will be higher using eVTOLs than using auto, the generalized travel cost will be less for commuters. On the other hand, with current eVTOL power requirement, the energy consumption and CO_2 emissions of AAM will be greater than those of auto driving, with an important contributor being the significance presence of empty flights relocation. These findings, along with sensitivity analysis, shed light on future eVTOL development to enhance the competitiveness of AAM as a viable option for commuting.

1. Introduction

Advanced Air Mobility, AAM, has been rapidly developing and attracted keen interest in the aviation and tech industries, academia, governments, and the general public as a time-saving travel solution for mobility in metropolitan areas. The traditional heavy reliance on passenger cars presents a perennial traffic congestion problem in many large metropolitan regions, causing exceedingly long travel time, especially for commute travel. In the US, for example, an average driver experienced 102 h of traffic delay in New York City and Chicago in 2024 [1]. Globally, millions of hours are lost each day due to traffic congestion [2,3]. AAM, by using electric vertical takeoff and landing (eVTOL) aircraft, offers a potential to transform personal mobility in metropolitan areas by expanding the travel dimension from 2D (on the ground) to 3D (on the ground plus in the air).

The successful deployment of AAM hinges first on its economic feasibility, especially in comparison with ground transportation. The earliest comparison may date back to Uber Elevate [4], which provides initial estimates of per vehicle-mile cost of VTOLs on a single trip basis. This pioneering study concludes that VTOL services is not likely to be cost competitive compared to driving for metropolitan travel in the near term, but has the potential to become a viable alternative. From the eVTOL vehicle design and optimization perspective, Brown and Harris [5] investigate the main cost drivers of AAM operations. A case study of airport access in New York City is conducted to evaluate AAM trip time and cost. The study argues that AAM may provide a cost advantage over current helicopter services but would be more expensive than car ride-sharing. More recently, Liu and Gao [6] perform a techno-economic analysis of eVTOL for urban air taxi services, by using a return-on-investment framework to assess its cost-revenue dynamics. The authors find that a positive rate of return is likely to be achieved based on realistic assumptions of critical parameters such as price per kilometer.

While these studies contribute to the understanding of the economic feasibility of AAM, no research has specifically looked into the economic feasibility of AAM for commuting. In metropolitan areas, commuters have long experienced significant traffic delays along with the stress of navigating crowded roadways and the difficulty in search for parking. To address these challenges, AAM provides a promising

* Corresponding author.
E-mail address: bzou@uic.edu (B. Zou).

https://doi.org/10.1016/j.team.2025.03.001
Received 11 September 2024; Received in revised form 26 January 2025; Accepted 10 March 2025
Available online 22 March 2025

alternative. First, AAM circumvents most of the road traffic: commuters only need to drive between home and a nearby vertiport, where eVTOLs fly to and from the central business district (CBD) where jobs are located. Given the high job density of CBD, the distance between the CBD vertiport and home locations is likely to be short, making it feasible to cover via a brief walk trip. On the other hand, the directional nature of commuting demand suggests the need for relocating empty eVTOLs to better match eVTOL supply and commuter demand. The need for eVTOL relocation, along with the need for charging and parking, suggests that a holistic rather than a single trip-based approach should be taken to assess the economic feasibility of AAM for commuting.

In addition to economic feasibility, the energy and environmental implications of using AAM for commuting have not been investigated either. Given the rising concern of the energy efficiency and climate impact of transportation, understanding whether commuting by AAM instead of auto would bring energy and environmental benefits is critical to justify the potential use of AAM. An elaborate investigation of this question requires detailed consideration of both eVTOL scheduling plans and eVTOL flight profiles. However, to our knowledge, no such joint effort has been taken.

To fill these gaps, this study develops an optimization approach to solve for the optimal eVTOL scheduling plan by considering various plausible AAM operational and passenger travel constraints, including eVTOL seating capacity, vertiport operation limits, charging needs, and passenger time windows. It is assumed that at the beginning of a day or the night before, commuters submit their travel time windows–specified by the earliest departure time at the origin vertiport and the latest arrival time at the destination vertiport—to the AAM operator. Using the submitted information, the AAM operator optimizes its operation plan and returns to each commuter the schedule of the eVTOL flights reserved for him/her. Thus, what we envision is a reservation-based AAM system. Given that AAM is still under development, the exact operational mode of AAM remains uncertain. In this study, we focus on eVTOL operations between one vertiport pair, which is likely to represent how AAM may begin at an early stage. The studied problem serves as a building block and a foundation for understanding how AAM could perform in more complex operational environments that will emerge at later AAM development stages. When numerically implementing the optimization approach in the Chicago metropolitan area in the US, we examine different vertiport pairs and distinct eVTOL models using a number of problem instances with randomly generated demand, to gain a comprehensive understanding and insights about the prospect of AAM for commuting.

In the remainder of the paper, Section 2 reviews the relevant literature. Section 3 introduces a time-expanded network model, which seeks the optimal eVTOL operation plan while respecting the various operational and time window constraints. We implement the model in the Chicago metropolitan area, to explore the potential of AAM for commuting. To this end, Section 4 first presents the experiment setup, including AAM commuting demand and model parameter specifications. Section 5 then reports the numerical results, including AAM operating cost, commuter travel time, generalized travel cost, and the associated energy consumption and CO_2 emissions. The insights gleaned from the results are further discussed in Section 6, along with a conclusion and suggestions for future research.

2. Literature review and contributions of the present study

While the existing body of AAM research is wide covering aircraft design, travel demand estimation, flight trajectory control, air traffic management, scheduling, and so on, the most relevant area to our study is eVTOL scheduling and dispatching. Shihab et al. [7] propose operations management models for AAM operators to decide the type of schedule to offer, how to dispatch the eVTOL fleet, and scheduling operations such that operator profit is maximized. Ale-Ahmad and Mahmassani [8] model AAM operations as a capacitated location–allocation-routing problem with time windows. A mixed-integer program is formulated to address request acceptance/rejection/allocation to eVTOL flights, as well as eVTOL routing and scheduling, while also allowing for demand consolidation. In a package delivery context, Farazi and Zou [9] seeks Pareto-optimal eVTOL dispatching schedules, considering the trade-off between minimizing eVTOL operating cost and the community impact of eVTOL noise. Shon and Lee [10] tackles a high-level AAM planning problem to determine the number of eVTOLs, vertiport spaces, and chargers, together with lower-level operations to control eVTOLs' operational states in in-service, charging, idling, and relocation.

The scheduling of eVTOL flights depends on the supporting infrastructure, particularly vertiports where eVTOLs take off and land. Because of this, some research has tackled tactical-level eVTOL operation planning jointly with strategic-level infrastructure decisions such as the number, locations, and capacities of vertiports. Wang et al. [11] develop a mixed-integer second-order conic optimization approach with an adaptive discretization algorithm to plan vertiports combining a facility location structure, a queueing network, and a demand function. Because strategic-level decisions are involved, the model does not get into detailed daily scheduling of eVTOL flights. In Chen et al. [12], a vertiport location selection problem is investigated, by assuming AAM demand to be distributed over the whole metropolitan area. A novel variable neighborhood search heuristic is designed to very efficiently solve the problem. An integrated modeling framework for airport shuttle service is proposed by Lv et al. [13], where vertiport site selection, capacity design, eVTOL route planning, and fleet size design are considered in conjunction with eVTOL service level and scheduling.

Apart from the above studies, the vertiport location problem has also been tackled in Rajendran and Zack [14], where the optimal vertiport locations in New York City are identified by applying iterative constrained clustering to the taxi data in the city. Willey and Salmon [15] address the complexities of optimal vertiport placement, by representing the problem as a modified single-allocation p-hub median location problem along with subgraph isomorphism techniques and heuristic algorithms to solve the problem. Rath and Chow [16] also employ a modified single-allocation p-hub medium location framework to determine the vertiport locations with two objectives of maximizing air taxi ridership and revenue. More recently, Jin et al. [17] takes a robust optimization approach to determine vertiport locations while accounting for traveler mode choice and uncertainties in user demand.

As eVTOLs cannot fly to customer doorsteps, to complete a trip, traveling by AMM will involve ground travel for vertiport access/egress. Straubinger et al. [18] argue that vertiport access/egress as key factors to improve the attractiveness of AAM. As such, a multi-modal perspective has been taken by some studies for AAM operation planning. Lim and Hwang [19] employs a k-mean clustering approach to determine vertiport locations in the Seoul metropolitan area in South Korea. The authors highlight that depending on the number and locations of vertiports, vertiport access and egress ground travel times might dominate UAM total travel time. Shon et al. [20] plan on the optimal eVTOL fleet size and vertiport numbers using generalized cost models of AAM trip chains with multiple ground access modes. For using eVTOLs for package delivery, Perez et al. [21] adopts a two-leg system design where eVTOLs first carry packages from a central distribution point to a set of vertiports in the suburbs in a metropolitan area, where packages are relayed to a ground transportation mode for the second-leg delivery to final customers.

Based on the above review, this study aims to make three main contributions:

- First, we explore the problem of using AAM for commuting from a daily scheduling perspective. Compared to other types of travel, commuting is unique given the directional and peaking nature of demand. As such, relocating flights to balance eVTOL availability and travel demand is critical, which significantly increases the operating cost. We propose a time-expanded network model to characterize the dynamics of eVTOL operations in different states: in-service flying, relocation flying, charging, and parking, while respecting various eVTOL operational and commuter time window constraints.

- Second, we demonstrate an application of the model using real-world data from the US Census to examine the economic feasibility of AAM for commuting from multiple facets, including changes in vehicle operating cost, commuter travel time, and commuter generalized travel cost compared to auto commuting. The application, performed in the Chicago metropolitan area, reveals the operational patterns of eVTOLs to cater for the plausible AAM commuting demand. Different vertiport pairs and eVTOL aircraft models are examined while accounting for demand uncertainties, which yields rich insights about the economic potential of AAM for commuting.
- Third, the energy and CO_2 emission implications of AAM for commuting, which is crucial for public acceptance, is further investigated. An aerodynamic approach is employed for the computation of eVTOL energy consumption. We break down the energy use and CO_2 emission by in-service flying, relocation flying, and ground access and compare them with the alternatives of auto commuting using either gasoline or electric cars. The breakdown allows us to clarify the potentially misleading conclusion about the energy efficiency and environmental attractiveness of AAM relative to auto commuting.

3. Optimization model

This section presents a time-expanded network model for optimizing eVTOL operations for passenger commuting between a suburb vertiport and a CBD vertiport. The model looks at one day of eVTOL operations. The total operation time in a day considered in our model is divided into T equal-length time steps. The set of the time steps is denoted by $\mathbb{T} = \{1, 2, \dots, T\}$. Each time step $t \in \mathbb{T}$ corresponds to time period $[t\Delta, (t+1)\Delta)$, where Δ is the length of a time period.

As commuters, each passenger is assumed to have a time window for taking AAM, specified as between his/her earliest possible departure time from the origin vertiport and latest possible arrival time at the destination vertiport. To be consistent with the time characterization in the model, the earliest possible departure time and the latest possible arrival time are measured in time step. The network model is developed such that all passenger trips are made within the passenger time windows.

Given the plausible space restraints for building and operating a vertiport, we consider that vertiports have limited capacities. In addition, the capacity of a vertiport can differ by location (e.g., a suburb vertiport is likely to be larger than a CBD vertiport given that lands are typically cheaper and more available in the suburb). Furthermore, takeoff and landing pads can require a more robust design than parking and charging pads due to higher structural demands to withstand the eVTOL hovering power during takeoff and landing [22,23]. Consequently, two distinct capacities are specified at a vertiport: one for takeoff and landing and the other for parking and charging.

In optimizing the eVTOL operations, the decision variables include: the time step of each passenger to depart from a vertiport, the number of eVTOLs in various states – departing as an in-service flight, departing as a relocation flight, holding at a vertiport, and charging at a vertiport – at each time point $t \in \mathbb{T}$, and the takeoff and landing capacities at each vertiport in each time step. For the number of eVTOLs being charged, we separately count the number of eVTOLs after completing an in-service or a relocation flight, recognizing that the energy use of a flight will differ whether the flight carries passengers. This subsequently affects charging costs. For the takeoff and landing capacities, we consider that the given number of takeoff and landing pads of a vertiport can be flexibly allocated for takeoff and landing operations in each time step, to best accommodate the eVTOL operation demand. Table 1 outlines the notations for the sets, parameters, and decision variables used in the model.

The objective of the model, shown in (1), is to minimize the daily AAM operating cost, encompassing various expenses related to in-service and relocation flight operations, charging, aircraft depreciation, and vertiport capital.

$$\min \sum_{i\in\mathbb{V}}\sum_{t\in\mathbb{T}}\{\alpha_s \cdot s_{i,t} + \alpha_r \cdot r_{i,t} + \beta_s \cdot c^s_{i,t} + \beta_r \cdot c^r_{i,t}\} + \gamma \cdot M + \sum_{i\in\mathbb{V}} \delta_i \cdot (K^{d,l}_i + K^{p,c}_i) \quad (1)$$

The cost minimization is subject to seven sets of constraints:

1. *eVTOL seating capacity constraint*: Constraint (2) imposes the eVTOL seating capacity constraints. This constraint ensures that the number of passengers departing from the suburb vertiport to the CBD, or vice versa, in a time step does not exceed the available seating capacity provided by the departing eVTOL flights of the time step.

$$\sum_{p\in\mathbb{P}} x^p_t \le Q \cdot s_{i,t}, \quad \forall t \in \mathbb{T}, i \in \mathbb{V} \quad (2)$$

2. *Vertiport capacity constraints*: Constraints (3)–(6) regulate eVTOL operational limits due to vertiport capacity constraints. Specifically, constraint (3) ensures that the number of eVTOL flights taking off from each vertiport in a time step does not exceed the available takeoff capacity. Similarly, constraint (4) stipulates that the number of eVTOLs arriving at each vertiport in a time step does not exceed the available landing capacity. In this constraint, we count the number of arriving eVTOL flights in time step t by backtracking the number of eVTOL flights departing from the other vertiport in time step $t - t_f$. To do so, subscript $3 - i$ on the right-hand side of the constraint gives the index of the other vertiport (if $i = 1$, $3 - i = 2$; if $i = 2$, $3 - i = 1$).

$$s_{i,t} + r_{i,t} \le k^d_{i,t}, \quad \forall t \in \mathbb{T}, i \in \mathbb{V} \quad (3)$$

$$s_{i,t-t_f} + r_{i,t-t_f} \le k^l_{3-i,t}, \quad \forall t \in \{t_f + 1, t_f + 2, \dots, T\}, i \in \mathbb{V} \quad (4)$$

Constraint (5) ensures that the sum of available takeoff capacity and available landing capacity at a vertiport is equal to the takeoff and landing capacity at the vertiport in each time step. Constraint (6) requires that the sum of eVTOLs being held and charged do not exceed the parking and charging capacity at each vertiport in each time step. An implicit assumption in the two constraints is that each takeoff (landing) pad handles at most one eVTOL takeoff (landing) operation in a time step.

$$k^d_{i,t} + k^l_{i,t} = K^{d,l}_i, \quad \forall t \in \mathbb{T}, i \in \mathbb{V} \quad (5)$$

$$h_{i,t} + c^s_{i,t} + c^r_{i,t} \le K^{p,c}_i, \quad \forall t \in \mathbb{T}, i \in \mathbb{V} \quad (6)$$

3. *Design balance constraints*: Constraints (7)–(9) ensure the balance of eVTOL flow. In our model, we assume that all eVTOLs are charged immediately after completing a flight, based on the rationale that it simplifies the eVTOL operational process (which will be important at the early-stage AAM deployment) and ensures that an eVTOL will be ready for the next flight at the earliest possible time. Following this assumption, constraints (7)–(8) describes that an arriving eVTOL gets charged at a vertiport right after completing the flight (the flight can be either an in-service flight or a relocation flight).

$$s_{i,t-t_f} = c^s_{3-i,t}, \quad \forall t \in \{t_f + 1, t_f + 2, \dots, T\}, i \in \mathbb{V} \quad (7)$$

$$r_{i,t-t_f} = c^r_{3-i,t}, \quad \forall t \in \{t_f + 1, t_f + 2, \dots, T\}, i \in \mathbb{V} \quad (8)$$

Constraint (9) says that the eVTOLs being charged and held at a vertiport in a time step should either depart from the vertiport (as an in-service flight or a relocation flight) or continue being held in the next time step. In our model, we consider that charging after a flight takes one time step. The length of a time step is set to five minutes in our model. This consideration is supported by the speculation that eVTOLs are likely to be ready for the next flight after one time step of charging. For example, Lilium Jet (one of the two eVTOL models

Table 1
Notations used in the model.

Sets	Description
$\mathbb{T}$	Set of time steps: $\mathbb{T} = \{1, 2, \ldots, T\}$
$\mathbb{V}$	Set of vertiports - {suburb vertiport (1) and CBD vertiport (2)}
$\mathbb{P}$	Set of all passengers, $\mathbb{P} = \mathbb{P}_1 \cup \mathbb{P}_2$
Parameters	**Description**
t_f	eVTOL flight time (in time steps) between suburban and CBD vertiports
t_e^p	Earliest possible departure time (in time step) of passenger p from the origin vertiport
t_a^p	Latest possible arrival time (in time step) of passenger p at the destination vertiport
M	eVTOL fleet size
Q	eVTOL seating capacity
γ	eVTOL capital cost (\$/eVTOL/day)
α_s, α_r	Operating cost for in-service/relocation flight between suburban and CBD vertiport (\$/flight)
β_s, β_r	Charging cost for in-service/relocation flight between suburban and CBD vertiport (\$/charge)
δ_1, δ_2	Capital and operation cost for suburban/CBD vertiport (\$/space/day)
$K_1^{d,l}, K_2^{d,l}$	Takeoff and landing capacity (per time step) at suburban/CBD vertiports
$K_1^{p,c}, K_2^{p,c}$	Parking and charging capacity (per time step) at suburban/CBD vertiports
Decision variables	**Description**
x_t^p	Binary variable indicating whether passenger p departs from origin vertiport in time step t
$s_{1,t}, s_{2,t}$	Integer variables indicating the number of in-service flights departing from suburban/CBD vertiport in time step t
$r_{1,t}, r_{2,t}$	Integer variables indicating the number of relocation flights departing from suburban/CBD vertiport in time step t
$h_{1,t}, h_{2,t}$	Integer variables indicating the number of eVTOLs being held at suburban/CBD vertiport in time step t
$c_{1,t}^s, c_{2,t}^s$	Integer variables indicating the number of eVTOLs being charged at suburban/CBD vertiport in time step t, after completing an in-service flight
$c_{1,t}^r, c_{2,t}^r$	Integer variables indicating the number of eVTOLs being charged at suburban/CBD vertiport in time step t, after completing a relocation flight
$k_{1,t}^d, k_{1,t}^l$	Integer variables indicating the available takeoff/landing capacities at suburb vertiport in time step t
$k_{2,t}^d, k_{2,t}^l$	Integer variables indicating the available takeoff/landing capacities at CBD vertiport in time step t

considered in our numerical experiments) is reported to achieve a 60% charge in five minutes [24], which is more than enough to fly one flight in our numerical experiments.

$$h_{i,t-1} + c_{i,t-1}^s + c_{i,t-1}^r = s_{i,t} + r_{i,t} + h_{i,t}, \quad \forall t \in \{2, 3, \ldots, T\}, \forall i \in \mathbb{V} \tag{9}$$

4. *Initial eVTOL assignment constraints*: Constraint (10) stipulates that at the beginning of a day, all eVTOLs start from the suburb vertiport, given that 1) morning commuting is typically from the suburb to CBD and 2) the suburb vertiport is likely to be larger due to less space restraints and thus more capable of holding eVTOLs when not in operation. As such, the sum of in-service flights, relocation flights, and eVTOLs being held at the suburb vertiport in the first time step is set to the fleet size. No eVTOLs are in other states in this time step, as characterized by constraint (10).

$$s_{1,1} + r_{1,1} + h_{1,1} = M \tag{10}$$

$$s_{2,1} + r_{2,1} + h_{2,1} + c_{1,1}^s + c_{1,1}^r + c_{2,1}^s + c_{2,1}^r = 0 \tag{11}$$

5. *Final eVTOL assignment constraint*: Constraint (12) describes the final positioning and status of eVTOLs, which should be either in holding or in charging at the suburb vertiport in the last time step in a day. In the last time step in the operation time in a day, all eVTOLs must be at the suburb vertiport where the eVTOLs will start operations the next day. Thus, the total number of eVTOLs being held and being charged at the suburb vertiport in the last time step must equal the fleet size.

$$h_{1,T} + c_{1,T}^s + c_{1,T}^r = M \tag{12}$$

6. *Passenger time window constraint*: Constraint (13) ensures that each passenger's departure is scheduled exactly once within their specified time window. The possible departure time steps range between the earliest possible departure time step t_e^p and the latest possible departure time step, which is backtracked by subtracting the flight steps t_f from the latest possible arrival time step t_a^p.

$$\sum_t x_t^p = 1, \quad t \in \{t_e^p, t_e^p + 1, \ldots, t_a^p - t_f\}, \quad \forall p \in \mathbb{P} \tag{13}$$

7. *Decision variables domains*: This final set of constraints defines the domains for the decision variables used in the model. Constraint (14) specifies that each passenger departs from the origin vertiport within his/her time window. Constraint (15) specifies that all decision variables associated with eVTOL operations as well as those governing vertiport takeoff and landing capacities are non-negative integers.

$$x_t^p \in \{0, 1\}, \quad \forall t \in \{t_e^p, t_e^p + 1, \ldots, t_a^p - t_f\}, p \in \mathbb{P} \tag{14}$$

$$s_{i,t}, r_{i,t}, h_{i,t}, c_{i,t}^s, c_{i,t}^r, k_{i,t}^d, k_{i,t}^l \in \mathbb{Z}_{\geq 0}, \quad \forall t \in \mathbb{T}, i \in \mathbb{V} \tag{15}$$

4. Numerical experiments: setup

The optimization model of Section 3 is numerically examined for AAM commuting in the Chicago metropolitan area. Since our focus is on early stage of AAM deployment, we consider that eVTOLs operate between one vertiport in the suburb and one vertiport in the Chicago CBD. We examine two scenarios in terms of the suburb vertiport locations: one in Northern Cook County and the other in Lake County. For each scenario, two distinct eVTOL models are investigated. This section describes the setup of the numerical experiments. We begin by describing how AAM commuting demand is generated in Section 4.1. Then, we present the model parameter values in Section 4.2.

4.1. AAM commuting demand

Spatial distribution of demand: We consider two AAM commuting scenarios. The first scenario focuses on AAM servicing between a vertiport located in Northern Cook County, which is further north, and Chicago CBD, which is often referred to as the "Chicago Loop" (Fig. 1). The second scenario focuses on AAM servicing between a vertiport located in Lake County and Chicago CBD. Both Northern Cook County and Lake County have significant commuter traffic to Chicago CBD during peak hours. According to the Illinois Department of Employment Security [25], Northern Cook County presents the largest source of commuters to Chicago CBD, while Lake County presents the third largest.

To identify the spatial distribution of the high-income commuters, we resort to the Longitudinal Employer-Household Dynamics Origin–Destination Employment Statistics (LODES) and the American Community Survey (ACS) from the US Census [26,27]. The LODES data provide detailed worker information in the US, including the home and work locations at the census tract level. The ACS data document the

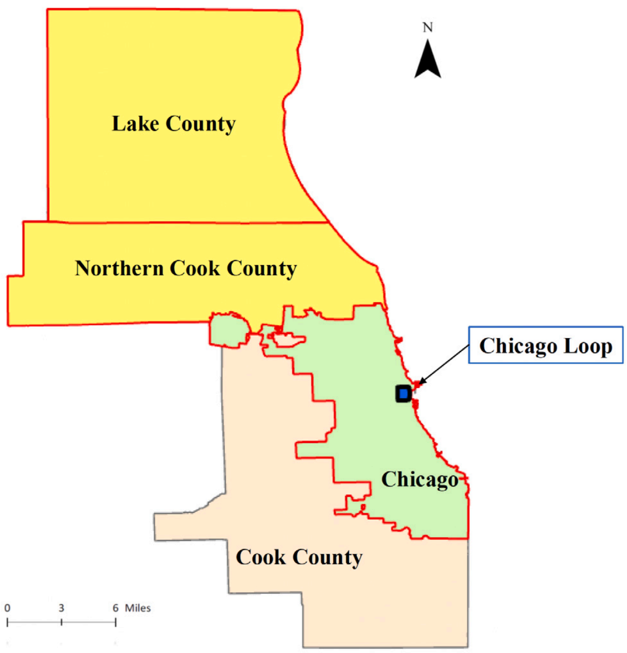

Fig. 1. The Chicago metropolitan area for numerical experiments.

percentage of residents in different income groups, also at the census tract level. In this study, we conjecture that commuters with a high income level are most likely to adopt AAM for commuting first. We set \$150,000 as the annual income threshold, above which commuters are considered to take AAM. We multiply the percentage of residents in a census tract with an annual income higher than this threshold by the number of workers who live in the census tract and work in Chicago CBD, to obtain an estimate of the number of potential AAM commuters between the census tract and Chicago CBD. In aggregate, the estimated numbers of potential AAM commuters are 2273 in Northern Cook County and 1317 in Lake County respectively.

Because the worker location information in LODES is specified only at the census tract level, we randomly generate a precise location within the home census tract of each potential AAM commuter as the home location of the commuter. Fig. 2 shows one instance of the generated home locations of the potential AAM commuters in Northern Cook County (a) and Lake County (b). For work locations, 145 workplaces are identified in Chicago CBD using Google Maps (Fig. 2(c)). For each potential AAM commuter, we randomly pick one out of the 145 workplaces as his/her work location.

While income is a critical determining factor, the willingness of commuters to use AAM also depends on how close the suburb vertiport is to home.[1] To this end, we consider that only those potential AAM commuters whose home locations are within a square zone of five square miles centered around the suburb vertiport will take AAM. Through a trial-and-error process, the suburb vertiport location for which the square zone encompasses the most potential AAM commuters is identified for each scenario, as shown in Fig. 2(a)-2(b). The CBD vertiport location is similarly determined. However, instead of looking into how many potential AAM commuters are encompassed, we seek to minimize the overall travel distance from the vertiport to the 145 identified workplaces. The CBD vertiport location is shown in Fig. 2(c).

Apart from distance, other factors can affect the propensity of a commuter to take AAM as well [28–30]. It is likely that not all commuters with an annual income above \$150,000 will take AAM. Conversely, some commuters even with a lower income may be willing to take AAM for commuting. As AAM has not been deployed for commuting, inherent uncertainties exist when predicting the AAM commuting demand. To partially capture the uncertainties, in the numerical experiments we generate and test 10 instances for each AAM commuting scenario. In each instance, the home and job locations (as well as the time window) of each AAM commuter are randomly generated within the commuter's census track in the suburb and in Chicago CBD. In Appendix B.3, we further experiment with higher demand levels, although the focus is on solution time. In addition to these efforts, more behavioral studies will be needed to better understand and forecast the AAM demand for commuting.

Temporal distribution of demand: Besides the spatial distribution, the temporal distribution of AAM commuter demand needs to be specified as well. As already described in Section 3, each AAM commuter has a time window for commuting characterized by the commuter's earliest possible departure time from the origin vertiport and the latest possible arrival time at the destination vertiport. Informed by the actual temporal pattern of commuter trips in a day [31], we assume that the earliest departure time of AAM commuters in each travel direction follows a truncated normal distribution: one between 6:00–10:00 AM (mean at 8:00 am) for commuting from the suburb to CBD; the other between 2:00–6:00 PM (mean at 4:00 pm) for commuting from CBD to the suburb, both with a standard deviation of 0.5 h. To illustrate, Fig. 3 displays the temporal distribution of earliest departure time of the commuters generated in Fig. 2 on the Northern Cook County-CBD route.

For each AAM commuter, we perform a random draw from each of the truncated normal distributions to generate the earliest departure time for morning and evening commutes. Considering that the length of a time step is set to five minutes in our numerical experiments, we convert the generated earliest departure time to the corresponding time step index. For example, if the generated earliest departure time for AAM commuter p is 6:47 am, it falls into the 10th time step starting from 6:00 am, i.e., $t_e^p = 10$. For the latest possible arrival time step t_a^p, it is obtained by adding a random number to t_e^p. Given that the it takes each AAM commuter about 15 min vertiport-to-vertiport on the Northern Cook County-CBD route and about 20 min on the Lake County-CBD route,[2] the random number is drawn from set $\{3, 4, 5, 6, 7, 8\}$ for the Northern Cook County-CBD route and from set $\{4, 5, 6, 7, 8, 9\}$ for the Lake County-CBD route. In other words, a value between 15 min and 40 min is added to the earliest possible departure time to obtain the latest possible arrival time on the Northern Cook County-CBD route. Likewise, on the Lake County-CBD route.

4.2. Model parameters

4.2.1. eVTOL models

Two eVTOL models are specified: Joby S4 and Lilium Jet (Fig. 4), which represent two distinct eVTOL aircraft designs. Joby S4 employs a conventional fixed-wing configuration with six tilting electric rotors, enabling smooth transitions between vertical and horizontal flight and accommodating four passengers plus a pilot. In contrast, Lilium Jet features a ducted fan propulsion system integrated into a canard wing configuration, with 36 electric ducted fans distributed across its wings. The emphasis of Lilium Jet on advanced fan integration contributes to its enhanced aerodynamic efficiency and payload—carrying up to six passengers plus a pilot. Both models utilize a vectored thrust configuration.

[1] In CBD, the area is dense and relatively small. As such, we assume that commuters will walk from the CBD vertiport to the work location.

[2] The vertiport-to-vertiport time for AAM commuters is calculated as the eVTOL flight time plus three minutes to capture commuter boarding/disembarking from the eVTOL. How eVTOL flight time is calculated is described in Section 4.2.2.

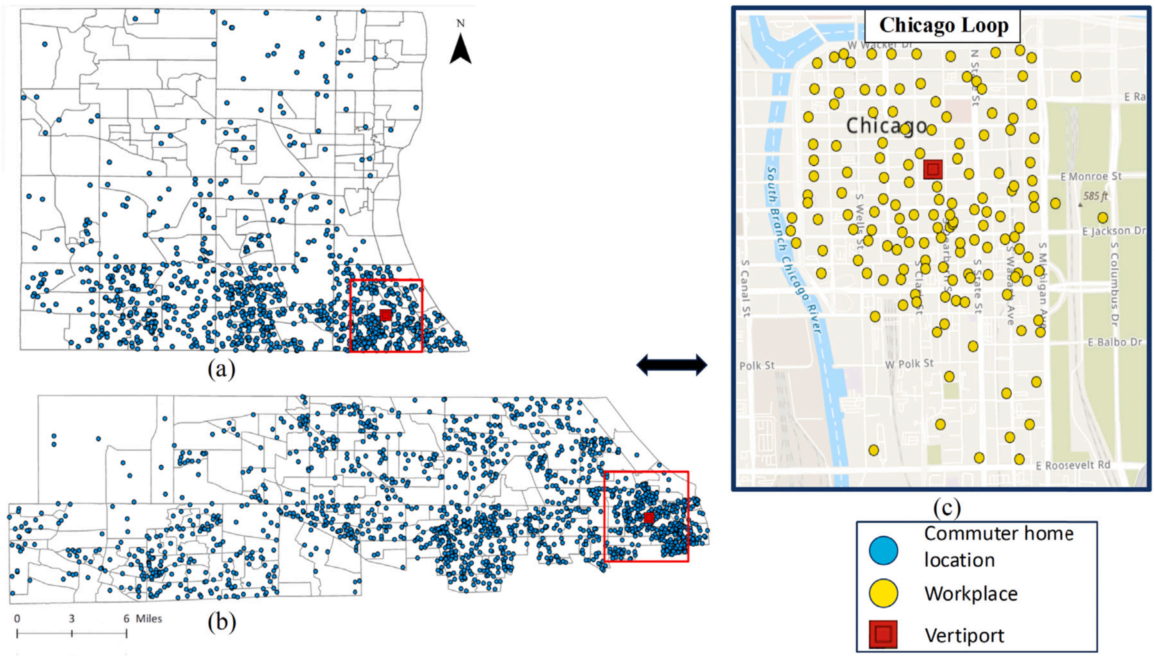

Fig. 2. (a) Home locations in Lake County, (b) home locations in Northern Cook County, and (c) work locations in Chicago CBD, generated for commuters with an annual income above $150,000.

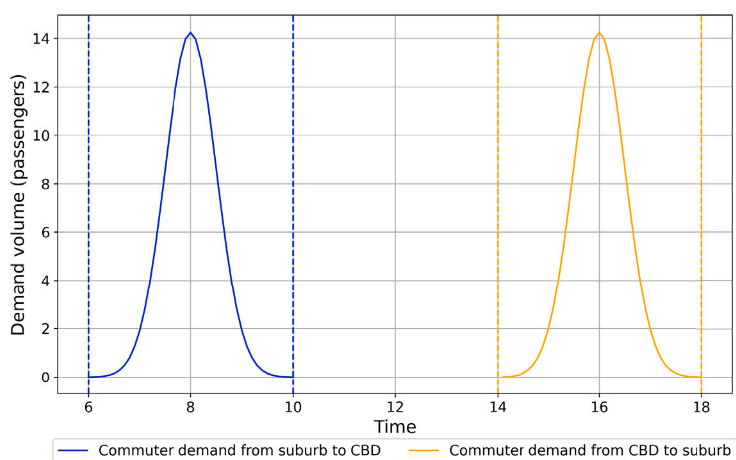

Fig. 3. Earliest departure time distribution of AAM commuters on Northern Cook County-CBD route.

Fig. 4. The two eVTOL models considered: (a) Joby S4 and (b) Lilium Jet.
Source: Vertical Flight Society [32,33].

4.2.2. eVTOL cost, energy use, and emission factors

The cost of an eVTOL flight consists of variable operating cost and capital cost. For variable operating cost, which includes crew and avionics cost, vehicle maintenance cost, and infrastructure cost, the estimates in [34] are adopted, at $366/hour for Joby S4 and $397/hour for Lilium Jet after excluding energy cost and capital cost. The energy cost is excluded as it is already counted in the charging cost in the objective function (1) of the optimization model. In addition, as we distinguish the energy use between an in-service flight and a relocation eVTOL flight, it is separately counting energy use for in-service and relocation flights. The capital cost is separately counted in our model as well, because our objective function (1) expresses capital cost as a function of the eVTOL fleet size. For capital cost, Joby S4 is estimated at $1,400,000 [33], while Lilium Jet at $7,000,000 [35]. The significantly greater cost of Lilium Jet can be attributed to its more complex and powerful propulsion system, more advanced aerodynamic design with a canard wing configuration, and a larger airframe.

Applying the above cost information to the study area, the values of the eVTOL cost parameters in the optimization model are derived. Specifically, the distance between the Northern Cook County vertiport and the CBD vertiport is 13 miles, while the distance between the Lake County vertiport and the CBD vertiport is 24.2 miles. Assuming an eVTOL cruise speed of 150 mph [4,36], we obtain the cruise time for an eVTOL flight. Apart from cruise, we further add two minutes for eVTOL climb and descent and one minute for takeoff and landing hovers to the total time of an eVTOL flight [37]. Then, the eVTOL flight time is multiplied by the variable operating cost per hour to obtain the variable operating cost per flight, at $50 for Joby S4 and $54 for Lilium Jet for flying on the Northern Cook County-CBD route, and at $77 for Joby S4 and $83 for Lilium Jet for flying on the Lake County-CBD route. Note that because energy cost is excluded, the variable operating cost per flight is considered the same for an in-service flight and a relocation flight. For capital cost per flight, we assume a service life of 30 years for eVTOLs, 260 operation days in a year, and a 3% discount factor. This results in a daily capital cost of $275 for Joby S4 and $1374 for Lilium Jet.

For energy use per eVTOL flight, we employ the approach in Kasliwal et al. [37]. For the interest of space, details about the approach are presented in Appendix A. On the Northern Cook County-CBD route, Joby S4 consumes 62.8 kWh for an in-service flight and 50.9 kWh for a relocation flight, while Lilium Jet uses 82.9 kWh and 66.3 kWh, respectively. On the Lake County-CBD route, Joby S4 requires 87.0 kWh for an in-service flight and 70.6 kWh for a relocation flight, while Lilium Jet consumes 115.0 kWh and 91.9 kWh, respectively. The energy cost per flight, which is captured by the charging cost after a flight in the optimization model, is then calculated using the average energy price in the state of Illinois, which is $0.10/kWh [38], multiplied by the energy consumed in a flight. For the Northern Cook County-CBD route, Joby S4 incurs a charging cost of $6.5 after an in-service flight and $5.3 after a relocation flight. Lilium Jet incurs a charging cost of $8.6 after an in-service flight and $6.9 after a relocation flight. For the Lake County-CBD route, Joby S4 incurs a charging cost of $9.1 after an in-service flight and $7.4 after a relocation flight. Lilium Jet incurs a charging cost of $12 after an in-service flight and $8.6 after a relocation flight. To calculate the CO_2 emissions of a flight, the energy used by a flight is multiplied by an appropriate emission factor. The emissions stem from electricity generation. In the state of Illinois, the emission factor of electricity generation is 0.314 kg CO_2/kWh.

4.2.3. Ground vehicle cost, energy use, and emission factors

As eVTOL cannot fly to passengers' doorsteps, using AAM for commuting still involves ground transportation for vertiport access/egress. At the suburban end, we assume that an AAM passenger will drive from his/her home to the suburb vertiport. At the CBD end, we consider that an AAM passenger will walk between his/her office building and the CBD vertiport. The latter consideration is reasonable given the small size and very high building density of the CBD area. Thus, to calculate the total energy use, accounting for the energy use of auto driving is needed. Moreover, as we desire to compare the cost, energy use, and CO_2 emissions of commuting by AAM and auto driving, obtaining appropriate ground vehicle cost, energy use, and emission factors will be necessary.

To this end, two types of cars are considered for auto driving: gasoline and electric. The gasoline car model is Toyota Corolla, with an operating cost of $0.63/mile for local travel and $0.59/mile for highway travel [39]. The electric car model is Tesla Model 3, which has lower operating costs of $0.44/mile for local travel and $0.42/mile for highway travel [40]. For energy use, Toyota Corolla has a fuel efficiency of 32 miles/gallon for local travel and 41 miles/gallon for highway travel [41]. Given that a gallon of gasoline contains 33.7 kWh of energy [42], the energy consumption rates for Toyota Corolla is 1.05 kWh/mile for local travel and 0.82 kWh/mile for highway travel. For Tesla Model 3, it can achieve a greater energy efficiency, at 0.29 kWh/mile for local travel and 0.32 kWh/mile for highway travel [43].

For CO_2 emission, Toyota Corolla has a tailpipe emission factor of 9.00 kg CO_2/gallon [44]. In addition, a 'well-to-use' emission factor of 2.14 kg CO_2/gallon [45] is incorporated to account for CO_2 emissions during production, refining, and transportation of the fuel before reaching the vehicle. To be consistent with the CO_2 emission calculation for eVTOLs, the two emission factors are combined, resulting in a total emission factor of 11.02 kg CO_2/gallon. Dividing this by the car's fuel efficiency gives emission factors of 0.34 kg CO_2/mile for local street travel and 0.27 kg CO_2/mile for highway travel. The CO_2 emission factor of Tesla Model 3 is obtained by multiplying its energy efficiency values by the emission factor of electricity generation in Illinois, which is 0.31 kg CO_2/kWh. This yields the CO_2 emission factors of Tesla Model 3 of 0.09 kg CO_2/mile for local travel and 0.10 kg CO_2/mile for highway travel.

4.2.4. Vertiport capital cost

The cost associated with vertiports consists of two parts: (1) capital cost and (2) operating cost. Recall in Section 4.2.2 that the eVTOL cost includes infrastructure cost which captures the expenses of operating vertiports. Therefore, only vertiport capital cost is specified here. Conceptually, the capital cost of a vertiport depends on the vertiport size. In this study, we make a simplification that the capital cost of a vertiport is proportional to the total number of pads (for takeoff/landing and parking/charging) the vertiport has. Thus, it is important to have an estimate of the capital cost per pad.

While existing estimates of vertiport capital cost are scarce, we follow Johnston et al. [46] which gives the capital cost of a medium-size vertiport with three takeoff/landing pads and six parking/charging pads to be $650,000. The capital cost per pad is obtained by dividing $650,000 by nine (which is the total number of pads). Since the objective function is about daily cost, we amortize the capital cost per pad, assuming a service life of 30 years, 260 operation days in a year, and a 3% discount factor. This yields a unit capital cost of $14.2 per pad per day.

The capital cost of a vertiport used in objective function (1) is then obtained by multiplying the unit capital cost above by the number of pads at the vertiport. Because all eVTOLs start operations from the suburb vertiport at the beginning of the day, the minimum number of parking/charging pads at the suburb vertiport is set equal to the eVTOL fleet size. Moreover, at the early stage of AAM deployment, eVTOL operations are expected to be in relatively simple and small in size. As such, we consider that a vertiport has two takeoff and landing pads to meet the minimum requirement of simultaneous takeoff and landing operations (i.e., one for takeoff and one for landing) in a time step. The total number of pads at the suburb vertiport is thus equal to the minimum number of parking/charging pads plus two. For the CBD vertiport, given the space constraint in CBD, we consider only three parking/charging pads in addition to the two takeoff/landing pads.

5. Numerical experiments: results

Now we proceed to implementing the optimization model in Section 3. The model, which is a mixed-integer linear program, is coded in Spyder Python 5.4.2 and solved using the SCIP optimization suite on a MacBook Pro with Intel Core i5 2.3 GHz dual-core processor and 8 GB of memory. Considering the randomness in AAM commuter demand, for each scenario 10 problem instances are randomly generated. Given an instance, we start from a large eVTOL fleet size and gradually reduce it, until a feasible solution cannot be obtained. In this process, we find that the objective function monotonically decreases. As such, we set the eVTOL fleet size at the minimum number that yields a feasible optimal solution.

In the rest of this section, the numerical results are mostly presented in the form of the average over the 10 generated instances for each scenario. When very detailed results such as travel time distribution of AAM commuters and flight operation schedules, only the results for the first generated instance are presented. The results for the other instances are not presented as they are very similar. All the instances can be solved very fast: for the Northern Cook County-CBD scenario, the solution time is within 26 s over all the 20 instances generated (10 instances times two eVTOL models); for the Lake County-CBD scenario, the solution time is within 22 s over all the 20 instances generated. Apart from the results reported in this section, sensitivity analysis is further conducted to investigate how the results change as values for some key parameters change. For the interest of space, details about the sensitivity analysis results are relegated to Appendix B.

5.1. Daily AAM operating cost

Fig. 5 shows the daily AAM operating cost averaged over 10 instances for each of the two scenarios. For each scenario, both Joby S4 and Lilium Jet are tested. Using Joby S4, the daily AAM operating cost is about \$27,300 for serving Northern Cook County-CBD and \$22,700 for serving Lake County-CBD, which are significantly lower (31.5% and 30.8%) than using Lilium Jet. The cost difference is mainly attributed to substantially higher capital cost of Lilium Jet (\$7,000,000 vs. \$1,400,000 for Joby S4). On the other hand, Lilium Jet enjoys a lower variable operating cost for both in-service and relocation flying due to its larger seating capacity and relatively comparable variable operating cost per flight.

Fig. 5 shows that the eVTOL variable operating costs incurred by in-service flights and by relocation flights are comparable. This can be attributed to two factors. First is the directional nature of commuter demand: in the morning from suburb to CBD and in the evening from CBD to suburb. In our numerical experiments, we observe that a relocation flight often occurs right after an in-service flight, which helps rebalance between eVTOL supply and commuter demand. This directional nature of commuter demand is further exacerbated by the limited space at the CBD vertiport, which contributes further to the need for eVTOL relocation. The considerable need for eVTOL relocation is illustrated in the distribution of eVTOLs in different states in Figs. 6–7.

Besides eVTOL variable operating cost, eVTOL charging cost and vertiport capital cost hold a small fraction in the daily operating expenses. In particular, the vertiport capital cost is almost negligible compared to the other cost items. The results suggest that the most important driving force for the economic feasibility of AAM is related to its operational efficiency, not much so about the capital investment in vertiports.

5.2. Travel time comparison with auto driving

A notable advantage of AAM for commuting is the potential travel time saving compared to auto driving. For each AAM commuter, we calculate the door-to-door travel time as the sum of: (1) travel time between home and suburb vertiport, (2) eVTOL flight time between the vertiports, and (3) travel time between work location and CBD vertiport. For travel between home and suburb vertiport, it is assumed that the commuter will drive. This travel time is calculated using Google Distance Matrix API, which incorporates historical traffic data to accurately estimate the driving time during peak hours. For auto commuting, the travel time is calculated in a similar fashion. The only difference is that driving lasts all the way from one's home to work location (or vice versa). The travel time between the two vertiports is eVTOL flight time plus three minutes which capture commuter boarding/disembarking from the eVTOL. For travel between the CBD vertiport and work location, the time needed is estimated using Google Maps, assuming a walking speed of 3 mph (4.8 km/h).

Recall that in this study, the proposed AAM for commuting system is a reservation-based system. Upon receiving the travel time window information from the commuters, the AAM operator runs the optimization model to generate an operation plan, including the departure time of each commuter from the origin vertiport. An AAM commuter will arrive at the origin vertiport right before its scheduled flight departure time. Consequently, waiting at the origin vertiport will be very minimum, thus neglected in our calculation.

Fig. 8 presents the distributions of door-to-door travel time of the commuters if they choose AAM vs. auto driving. The distributions are based on the first generated instance for each scenario. For the other instances, the distributions are similar and thus not presented for brevity. For Northern Cook County-CBD commute, Fig. 8(a) clearly shows that the travel time distributions of using AAM and auto driving do not have an overlap. All commuters will experience a travel time saving by taking AAM. The average door-to-door commute time by AAM is 30 min, as opposed to 56 min by auto, or 26 min of time saving. For Lake County-CBD commute, Fig. 8(b) shows an even larger disparity between the travel time distributions of using AAM and using auto. The average door-to-door commute time by AAM is 36 min, as opposed to 68 min by auto, or 32 min of time saving. Overall, using AAM cuts commute time by almost half.

It is worth noting that the calculation of the commute time does not directly rely on the optimization solution (as long as the solution accommodates all AAM commuter demand). The travel time saving results will be used together with the operating cost results from the optimization solution to come up with generalized travel cost for comparison between AAM and auto commuting. This is presented next.

5.3. Generalized travel cost comparison with auto commuting

Using the results from the previous two subsections, we proceed to calculating the generalized travel cost of AAM and auto commuting. For AAM commuting, the generalized travel cost of a commuter in a day, which involves a morning trip from home to work location and an evening trip from work location back to home, is composed of three parts. The first part is the daily AAM operating cost borne by a commuter, which is obtained by dividing the total daily operating cost by the number of commuters.[3] The second part is the auto operating cost associated with driving between home and the suburb vertiport. For illustration, here we assume gasoline cars for this part of driving. The cost is calculated by multiplying the per mile operating cost by the mileage between home and the suburb vertiport, times two (to account for morning and evening trips). The mileage information is obtained using Google Distance Matrix API.

For the third part, it is about the travel time-related cost, which relates to commuter value of time (VOT). We follow a recent estimate of Boddupalli et al. [29], who provide separate traveler VOT distributions while taking eVTOL, driving, and out-of-vehicle. Assuming

[3] This part could be more accurately measured as the fare paid by commuters to take eVTOL. However, as this study does not deal with AAM pricing, we use AAM operating cost borne by a commuter as a proxy.

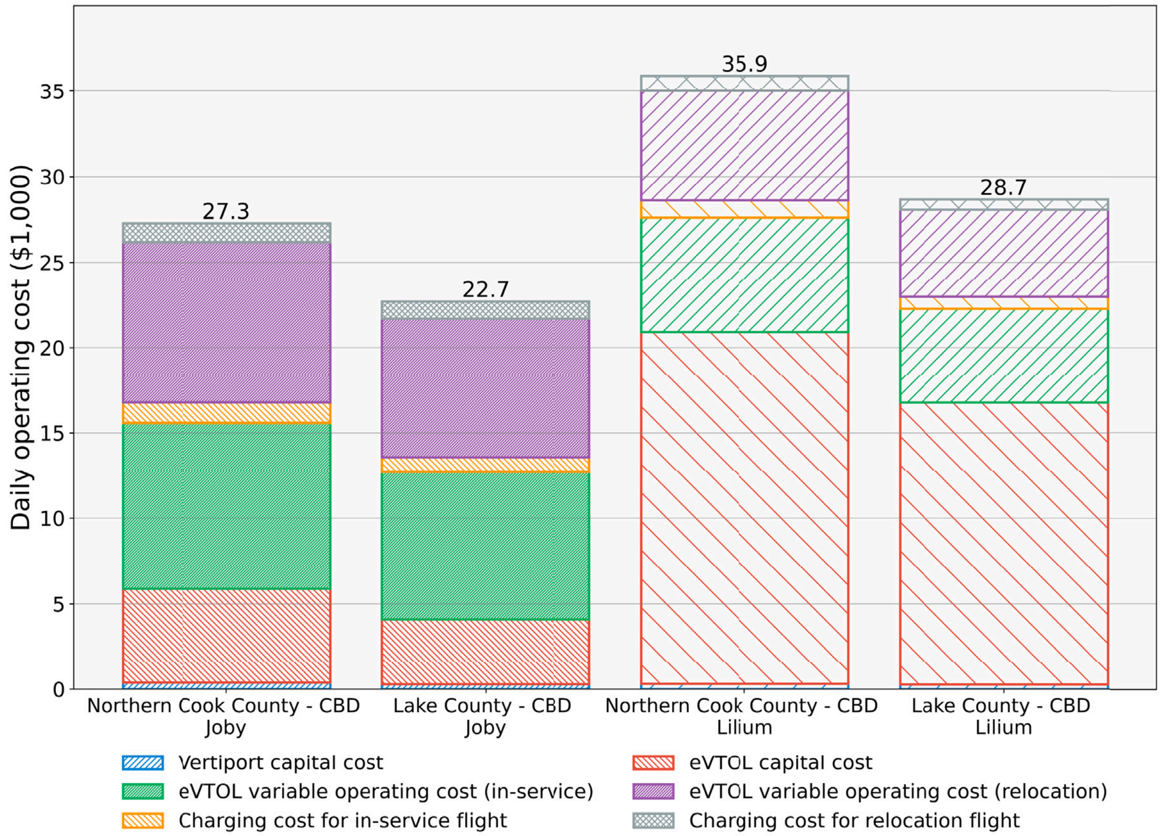

Fig. 5. Daily operating cost for AAM commuting.

that higher-income travelers are associated with higher VOTs, we first identify the percentage of the commuters with income greater than $150,000 in the overall commuter population based on the LODES data. We find that these commuters account for the top 6.5% on the Northern Cook County-CBD route and the top 8.5% on the Lake County-CBD route. Given these percentages, we pick the 95th percentile value in each of the three VOT distributions as the average VOT of the AAM commuters while taking eVTOL, driving, and out-of-vehicle (which in our context is walking). For a commuter, these VOT values are multiplied by the amount of time spent in taking eVTOL, driving, and walking, and then summed together to yield the travel time-related cost.

For auto commuting, the generalized travel cost of a commuter is calculated in a similar way. The auto operating cost is derived by multiplying the per mile operating cost specified in Section 4.2.3 by the mileage on local streets and highways that a commuter incurs in a day. The mileage information is again obtained from Google Distance Matrix API. As both gasoline and electric are considered, two operating costs are calculated for auto commuting. The travel time-related cost is calculated by multiplying the traveler VOT for driving by the amount of time spent if driving door-to-door between home and work location.

Fig. 9 displays the generalized travel cost per commuter in a day, averaged over all AAM commuters and all the generated instances. In each commuting scenario, four bars are presented: AAM commuting using Joby S4, AAM commuting using Lilium Jet, auto commuting by gasoline car, and auto commuting by electric car. We can see that for both Northern Cook County-CBD and Lake County-CBD commuting, the vehicle operating cost is always significantly higher using AAM. The higher vehicle operating cost is offset by the lower travel time-related cost using AAM. Overall, the generalized travel cost per commuter in a day will be lower by AAM than by auto. In particular, using Joby S4 yields the lowest generalized travel cost, which is about 22%–25% lower than if using gasoline cars in the two commuting scenarios.

5.4. Energy consumption and CO_2 emissions

We apply the energy and emission factors described in Sections 4.2.2–4.2.3 to the optimization results to compute the energy consumption and CO_2 emissions when AAM is used for commuting. For comparison, the energy consumption and CO_2 emissions by auto commuting are also calculated. Fig. 10 reports the total energy use results: the colored solid bars show the averages of the generated instances, while the error bar at the top of each solid bar displays the range of the total energy use from the individual generated instances. Overall, the error bars are short, suggesting consistency of the results across the different instances. Considering that we have two eVTOL models and two types of cars (gasoline and electric), the energy consumption is calculated for six cases: four involving AAM and two for auto commuting. For AAM commuting, the energy consumption is broken down into the energy used by in-service eVTOL flights, relocation eVTOL flights, and ground mode (auto), which corresponds to driving between home and the suburb vertiport.

Three observations are worth discussing. First, regardless of the commuting scenarios and the eVTOL models, AAM commuting always consumes substantially more energy than auto commuting. Compared to cars which travel on the ground, flying in the air requires substantially more energy not only for cruise but also for takeoff hover, landing hover, climb, and descent. These non-cruise phases account for a significant portion of the energy use of an eVTOL flight [21]. The difference in energy consumption is particularly prominent if electric cars are used for commuting.

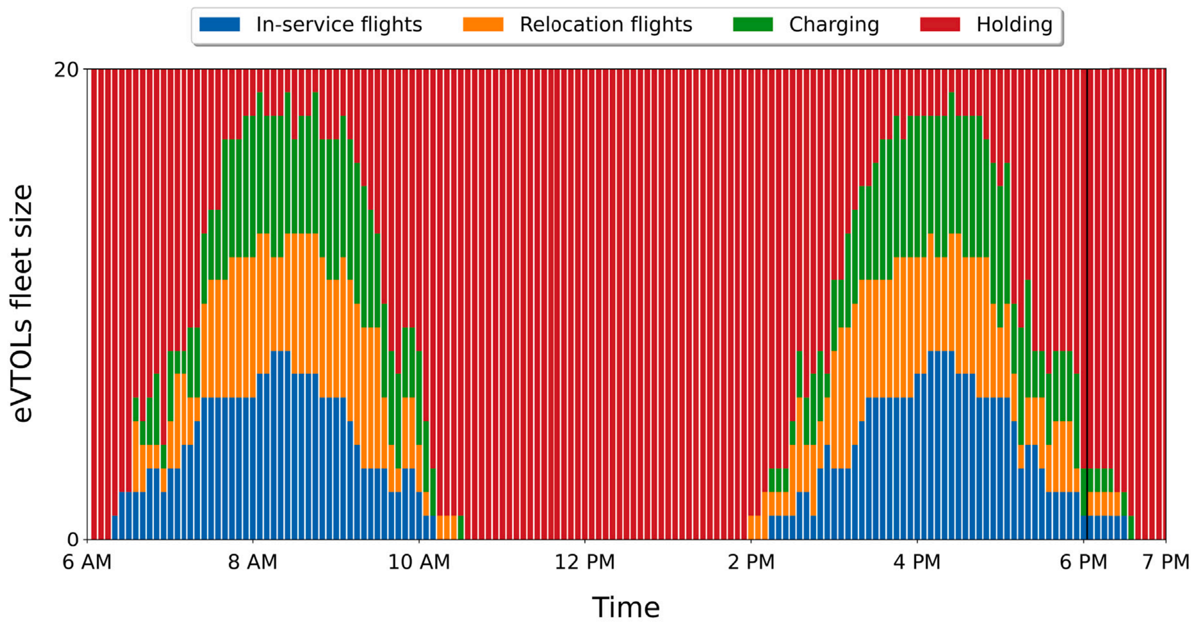

(a) Joby S4

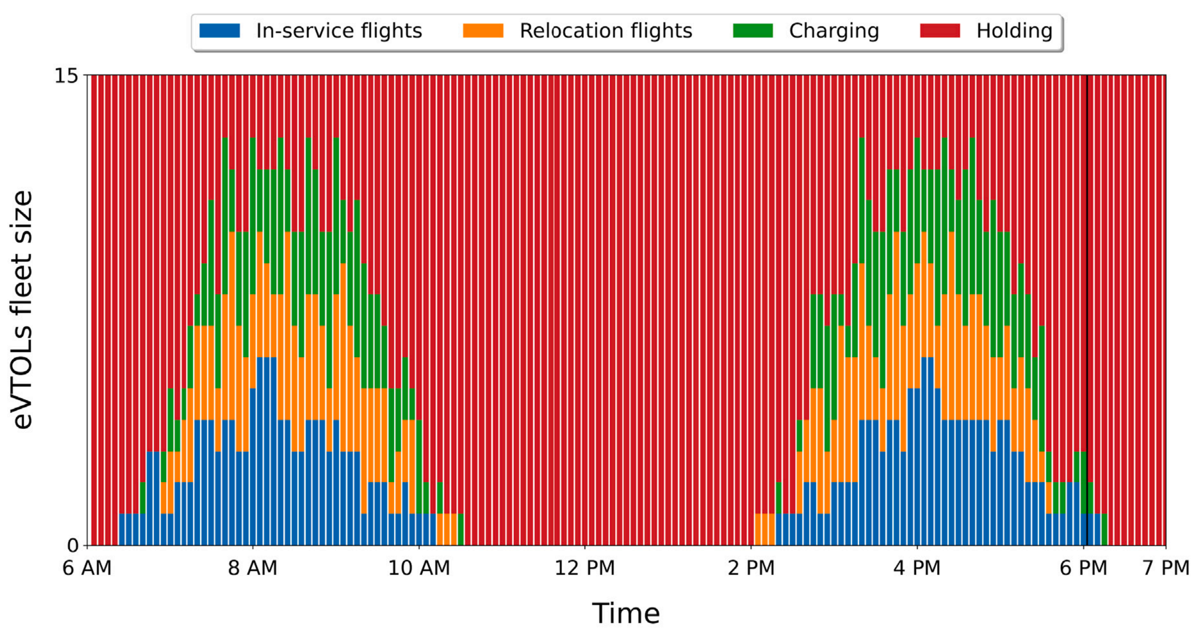

(b) Lilium Jet

Fig. 6. eVTOL operations on Northern Cook County-CBD route.

Second, relocation eVTOL flights consume about the same energy as in-service flights. Together, relocation and in-service flights hold the bulk of the total energy consumption, whereas ground travel between home and the suburb vertiport account for only a small fraction. If we just look at the energy consumption from in-service flying and ground travel for vertiport access, the energy use of AAM commuting is lower than auto commuting by gasoline car. For people not thinking carefully enough about the AAM operational details, this could lead to an incorrect conclusion that using AAM for commuting would be energy attractive. However, this ignores the crucial fact that, due to the inherently unbalanced nature of commute traffic and space limit at a CBD vertiport, eVTOL relocation is necessary and results in a much higher total energy consumption for AAM commuting.

Third, between Lilium Jet and Joby S4, using Lilium Jet leads to lower energy consumption. While a single Joby S4 flight requires less energy than a single Lilium Jet flight, as is shown in Section 4.2.2, a Lilium Jet flight has 50% greater seating capacity. As a consequence, per seat energy consumption for Lilium Jet is lower. The larger seating capacity of Lilium Jet also means fewer flights to accommodate the same AAM commuting demand. Overall, the energy consumption using Lilium Jet is less than the energy consumption using Joby S4.

Fig. 11 shows the CO_2 emission results. Given the close association between energy consumption and CO_2 emissions, it is not surprising that the relativity of the CO_2 emissions resembles that of energy consumption in Fig. 10. AAM commuting emits more CO_2 than auto commuting. Among the four cases of AAM commuting, Lilium Jet +

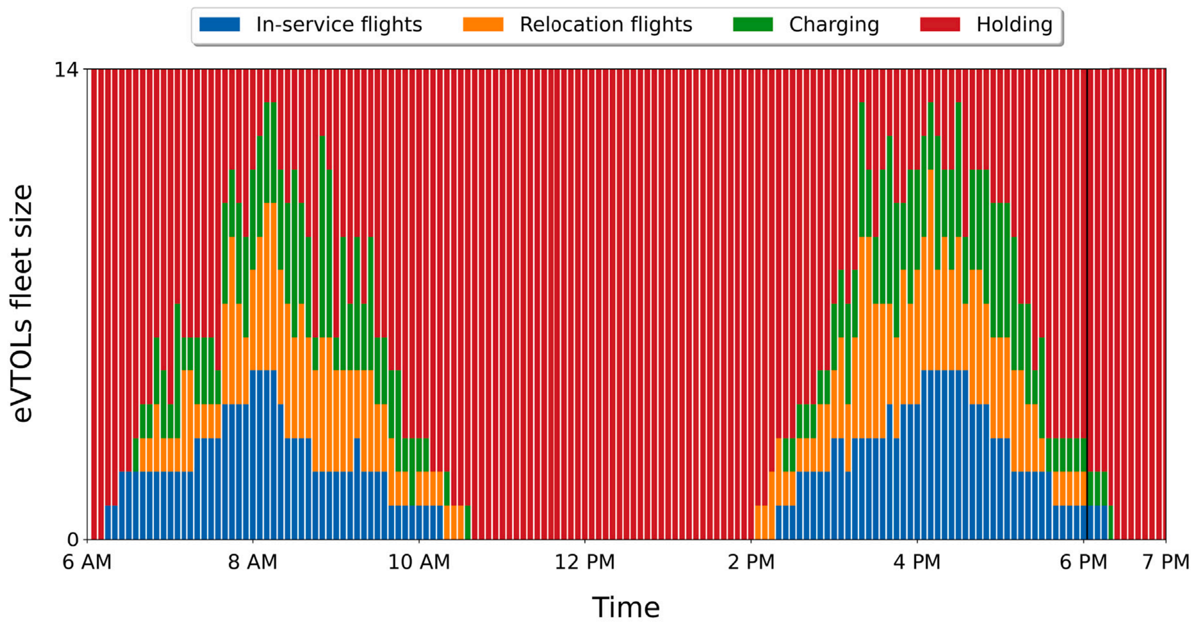

(a) Joby S4

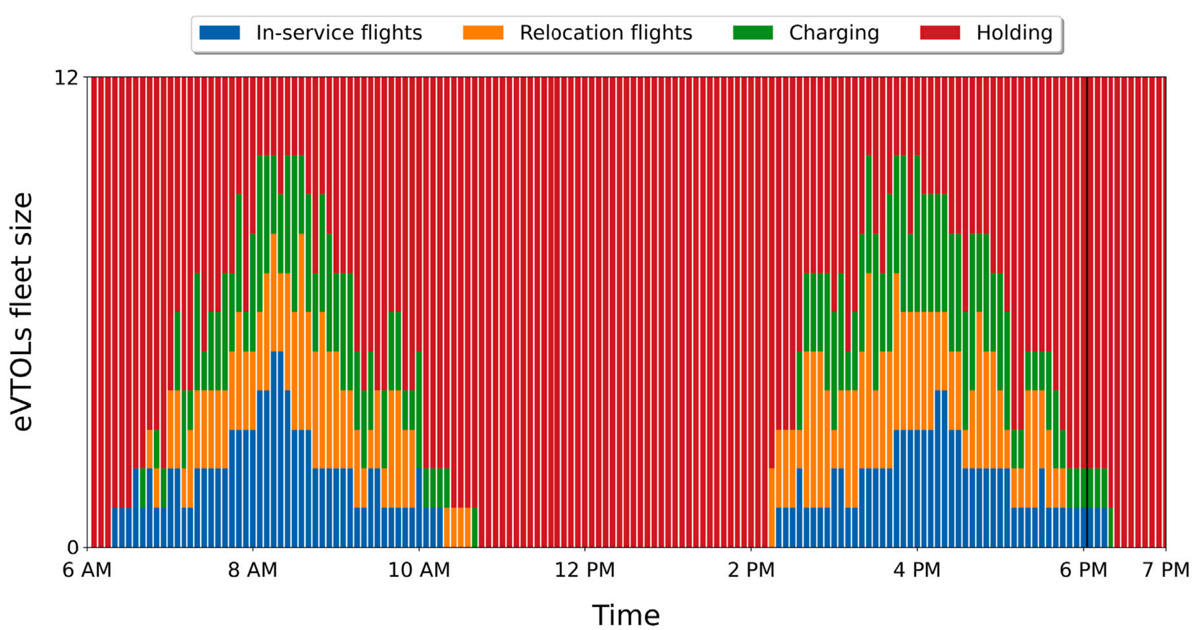

(b) Lilium Jet

Fig. 7. eVTOL operations on Lake County-CBD route.

electric car as the ground mode results in the least emission. Still, it is significantly higher than using auto for commuting. Overall, AAM commuting does not seem to be more attractive than auto commuting in terms of energy consumption and CO_2 emissions, at least with the current eVTOL performance.

6. Discussions and conclusion

The numerical experiments provide several insights into using AAM for commuting in a metropolitan area. First, the most significant driver for using AAM to commute is the potential savings in travel time. Our numerical results demonstrate that all commuters will experience a sizable reduction in travel time. Moreover, the longer the commuting distance, the greater the travel time saving that AAM can bring compared to auto driving, which is clearly shown by the separation of the travel time distributions between using AAM and using auto in the two commuting scenarios (Fig. 8). Thus, from the travel time reduction perspective, AAM may be more attractive for commuters who live farther away from their work locations.

Second, eVTOLs are likely to be expensive to own and operate, at least in the early stage of AAM deployment. As such, using AAM will incur greater vehicle operating cost than using auto for commuting, even with the fact that an eVTOL flight can carry multiple travelers and only one traveler in the car for auto driving. The significant need for

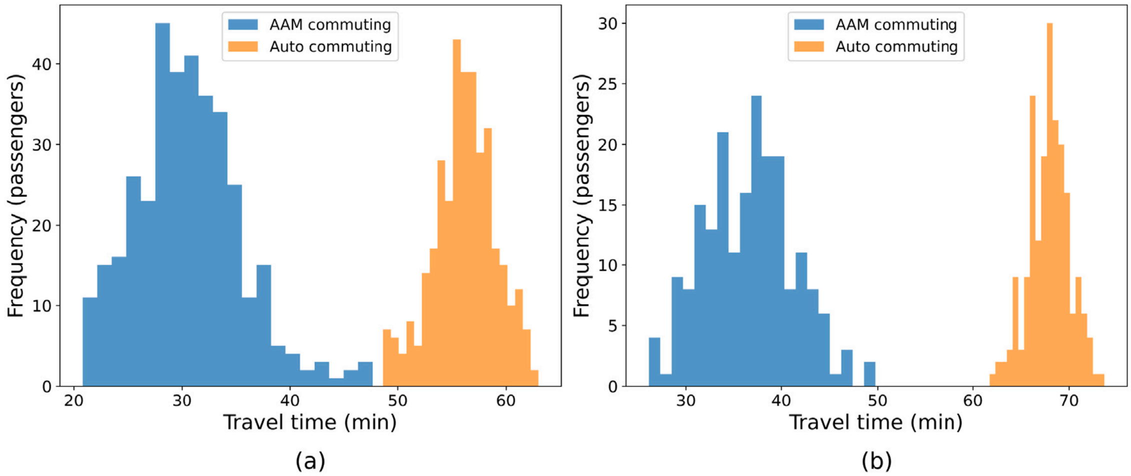

Fig. 8. Travel time distributions for AAM and auto commuting: (a) Northern Cook County-CBD and (b) Lake County-CBD.

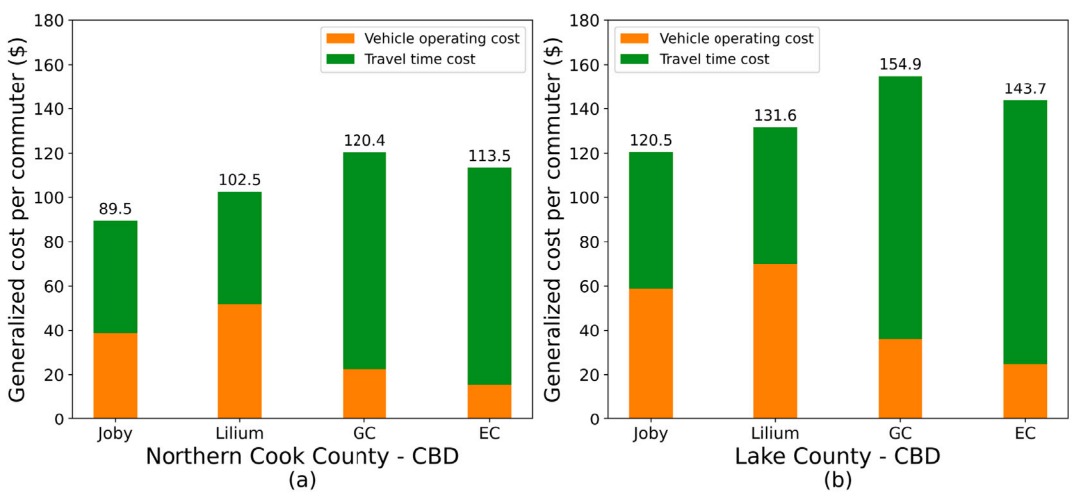

Fig. 9. Generalized travel cost per commuter (GC: gasoline car; EC: electric car).

eVTOL relocation—due to the inherent directional nature of commuter demand, adds to the eVTOL operating cost and exacerbates the cost difference with respect to auto commuting. Therefore, continuous improvement of eVTOL cost efficiency is needed to economically justify its potential use for commuting. To recover the operating cost, AAM operators may also explore revenue-generating opportunities using the empty seats on the relocation eVTOL flights, for example, letting relocating flights carry packages for delivery [9].

Third, when it comes to the generalized travel cost, the travel time saving benefit from taking eVTOL dominates over the effect of higher operating cost of eVTOL than auto driving. As a result, using AAM for commuting leads to a lower generalized travel cost per commuter. The generalized cost reduction could justify government support in the forms of R&D investment and subsidy to bring the eVTOL cost down and accelerate the AAM deployment. This can help reduce the operating cost of eVTOLs, which in turn attracts more travelers to use AAM. More travelers could create economies of scale which further brings down the eVTOL operating cost, thus a positive feedback loop.

Fourth, due to the significantly greater power requirement by eVTOLs to fly than by cars to travel on the ground, AAM for commuting will consume more energy and produce more CO_2 emissions than auto driving. Future R&D efforts should focus on enhancing the energy efficiency of eVTOLs. This will involve a multi-faceted approach encompassing aerodynamic, structural, battery, and propulsion advancements in eVTOL design. For example, the more streamlined airframe of Lilium Jet than Joby S4 can be a contributor to the reduced energy use. In addition, understanding the relationship between eVTOL power requirement and seating capacity is also needed to design the right-sized eVTOL aircraft with the best energy and environmental performance.

Finally, the comparison between Joby S4 and Lilium Jet, reveals the relative attractiveness of the two eVTOL models. Joby S4, with its simpler aerodynamic design and propulsion system, enjoys a significantly lower capital cost than Lilium Jet. This presents the main contributor to the smaller operating cost and generalized commuter travel cost by using Joby S4 for commuting. Despite the slightly higher energy consumption, Joby S4 is likely to be the choice for AAM operators. Beyond Joby S4 and Lilium Jet, more eVTOL models, especially those with distinct performance parameters, can be further investigated to identify the best eVTOL model and inform potential aircraft refinement.

This research presents a start toward understanding the potential of using AAM for commuting in metropolitan areas. A service network design model is developed to schedule eVTOLs to fly between two vertiports, one in the suburb and one in the in CBD, while respecting the operational constraints such as vertiport capacity limit and commuter time windows. Several interesting insights are generated from

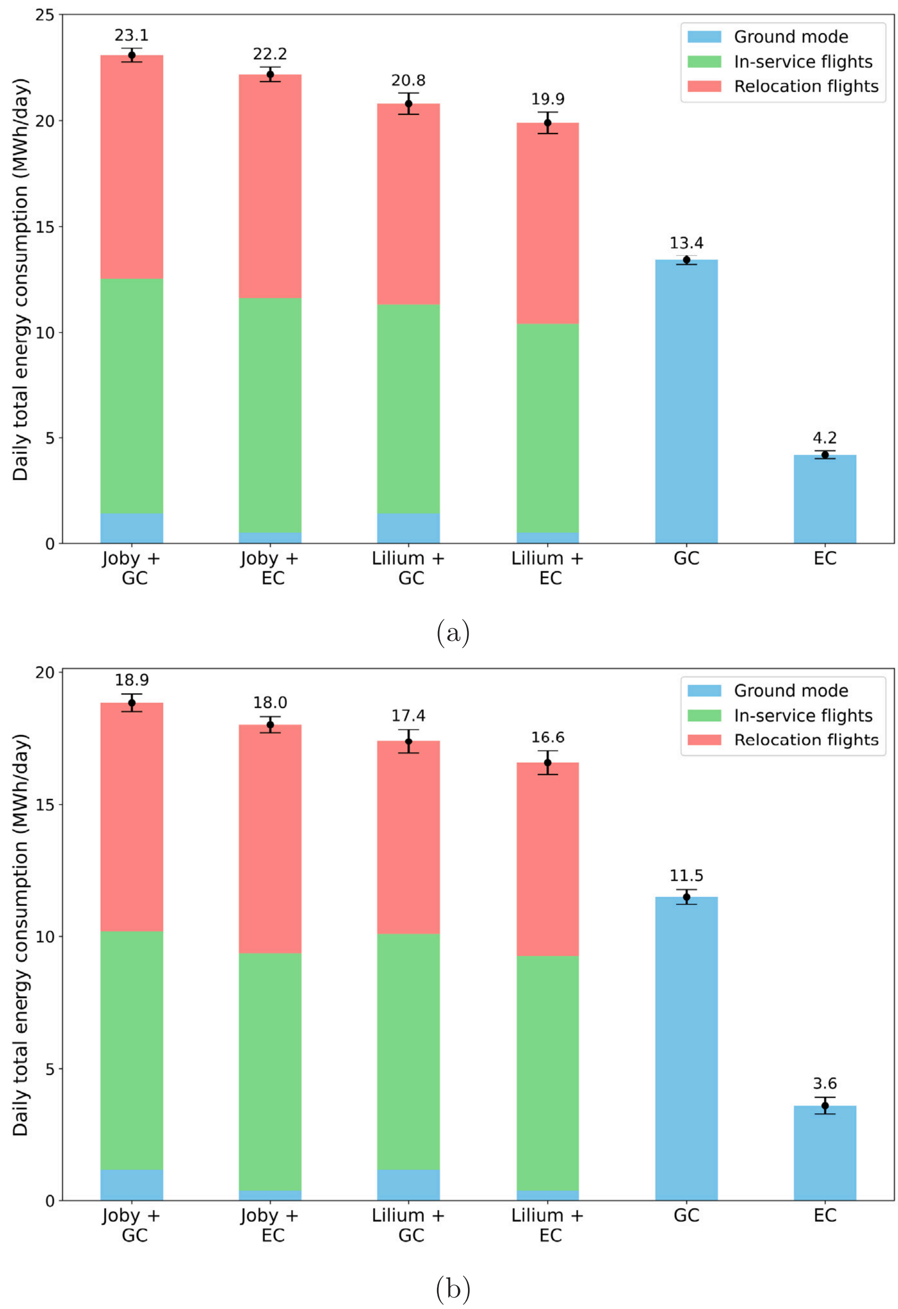

Fig. 10. Comparison of energy consumption on (a) Northern Cook County-CBD route and (b) Lake County-CBD route (GC: gasoline car; EC: electric car).

the numerical experiments by implementing the model in the Chicago metropolitan area, which can be used to inform future eVTOL design and AAM deployment, to enhance the competitiveness of AAM as a viable option for commuting.

We suggest a few directions as possible extensions of the present research. First, this study considers AAM commuting between two vertiports. While it is likely to be the case at an early stage of AAM deployment, over time this new mode of transportation is expected to become more accepted by commuters. Consequently, the AAM operator will expand its service beyond one vertiport pair. Future research can be directed to the modeling and possibly tailored algorithm development to deal with a multi-OD service network, e.g., by connecting CBD to multiple suburbs. Second, the extent to which the CBD vertiport capacity constrains eVTOL operations can be further investigated. With limited space, a vertiport in CBD is expected to be small in size. Future research may explore having multiple vertiports at CBD, e.g., setting up vertiports on the rooftops of multiple high-rise buildings. Third, while the use of discrete time steps in a time-expanded network allows for absorbing operational uncertainties (e.g., if the eVTOL flight time deviates from the nominal flight time by a couple of minutes, it is likely that the time step for eVTOL arrival remains unchanged), it would be helpful to investigate additional ways, such as robust optimization, to account for the uncertainties. Lastly, in this research, we consider potential AAM commuters to be those with an annual income above a threshold. While this is probable, it is also possible that lower-income commuters have an interest in taking AAM to work. To this end, more elaborate behavioral studies will be needed to better understand and characterize the demand side of AAM commuting, including what and how socioeconomic and AAM operational factors influence the mode choice of commuters.

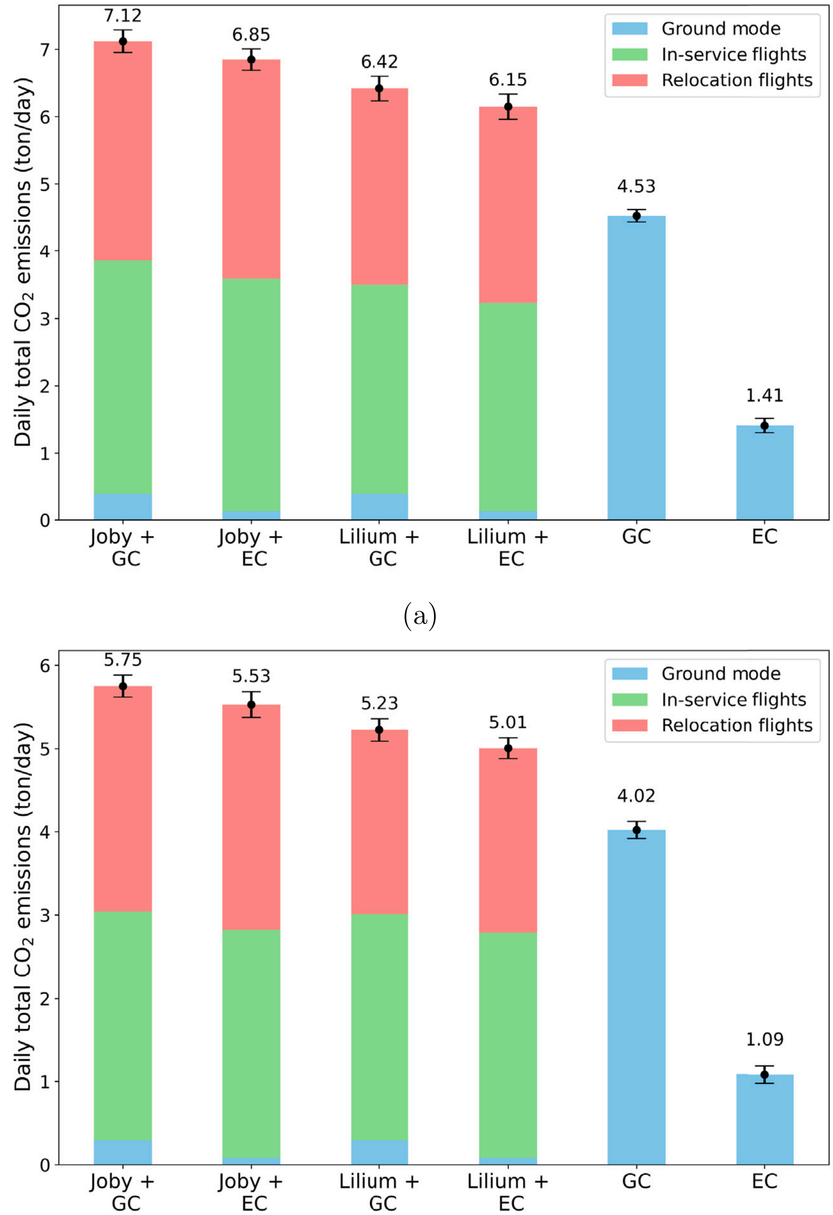

(a)

(b)

Fig. 11. Comparison of CO_2 emissions on (a) Northern Cook County-CBD route and (b) Lake County-CBD route (GC: gasoline car; EC: electric car).

CRediT authorship contribution statement

Daniel Perez: Writing – original draft, Visualization, Methodology, Investigation, Formal analysis, Data curation. **Heeseung Shon:** Writing – review & editing, Validation, Supervision, Methodology, Investigation. **Bo Zou:** Writing – review & editing, Validation, Supervision, Resources, Methodology, Funding acquisition, Conceptualization. **Kenneth Kuhn:** Writing – review & editing, Validation, Supervision.

Declaration of competing interest

None.

Acknowledgment

This research was supported in part by the US National Science Foundation (NSF) under grant numbers 2112650 and 2330565. The support of the NSF is gratefully acknowledged. The authors would also like to thank the anonymous reviewers for their insightful and constructive comments, which helped us further strengthen the paper.

Appendix A. Calculating energy use of an eVTOL flight

An eVTOL flight profile is composed of five phases: takeoff hover, climb, cruise, descent, and landing hover (Fig. A.12). Thus, the energy use of an eVTOL flight is the sum of energy use in the five phases. In each phase, the energy use is calculated as the required power multiplied by the time spent in the phase. In doing so, three assumptions are made [21,37]. First, the takeoff hover and the landing hover phases have the same energy requirements. Second, the additional energy required during climb as compared to cruise due to acceleration is approximately counterbalanced by the energy savings during descent compared to cruise due to deceleration. Consequently, assuming cruise performance for the whole duration of climb and descent is a good

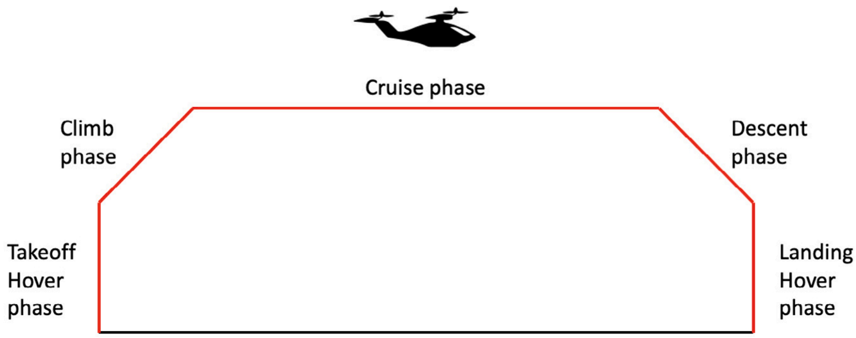

Fig. A.12. eVTOL flight profile.

approximation. Third, we assume that an eVTOL cruises at an altitude of 1000 ft, with the rate of climb/descent at 1000 feet/minute.

The power during the hover phases, referred to as hover power, is calculated as:

$$P_{\text{hover}} = \frac{wg}{\eta_h}\sqrt{\frac{\delta}{2\rho}} \tag{A.1}$$

where w is the eVTOL weight, g is gravity constant, η_h is hover system efficiency, δ is disk-loading, and ρ is sea-level air density.

The power during the cruise phase, referred to as cruise power, is calculated as:

$$P_{\text{cruise}} = \frac{mg}{\frac{L}{D}}\frac{v}{\eta_c} \tag{A.2}$$

where v is cruise speed, L/D is the lift-to-drag ratio (L stands for lift, the force that holds the eVTOL aloft; D stands for drag, the aerodynamic resistance the eVTOL encounters while moving through the air), and η_c is cruise system efficiency. We calculate the cruise power to determine the amount of energy required for an eVTOL to sustain steady-level flight at its cruising speed.

With Eq. (A.1)–(A.2), the total energy consumption for an eVTOL flight is calculated as follows:

$$E = \frac{2 \cdot P_{\text{hover}} \cdot t_{\text{hover}} + P_{\text{cruise}} \cdot (t_{\text{cruise}} + 120)}{3600 \cdot CD \cdot PD} \tag{A.3}$$

In the above equation, t_{hover}, set at 30 s for both the takeoff hover and the landing hover phases. For cruise time, two additional minutes (120 s) are added to account for the climb and descent phases as per the second assumption. CD is the battery charge–discharge efficiency. PD is primary-to-delivered electricity efficiency. In the denominator, 3600 converts the calculated energy from kilowatt-seconds (kWs) to kilowatt-hours (kWh).

It should be noted that following the above equations allows us to distinguish the energy use between an in-service flight and a relocation flight by using different m's. For Joby S4, the maximum gross weight is 2404 kg. Assuming that the average weight of a pilot/passenger is 90 kg, the empty weight of Joby S4 is 1950 kg. Similarly, Lilium Jet has a maximum gross weight of 3175 kg with an empty weight of 2539 kg. For an in-service flight, it is assumed that all seats are occupied, i.e., the maximum gross weight is used for m.[4] For relocation flights, only the pilot's weight is added to the empty weight to obtain m. The parameters and their values in Eqs. (A.1)–(A.3) are summarized in Table A.2.

Table A.2
Parameters values for eVTOL aircraft energy calculation.
Source: Vertical Flight Society [32,33],Zhang et al. [36],Kasliwal et al. [37].

Parameter	Symbol	Value (Unit)
Joby S4 maximum gross weight	m	2,404 kg
Joby S4 empty weight	m	1,950 kg
Lilium Jet maximum gross weight	m	3,175 kg
Lilium Jet empty weight	m	2,539 kg
Gravitational acceleration	g	9.81 m/s^2
Cruise speed	v	150 mph (67.1 m/s)
Hover system efficiency	η_h	0.63
Cruise system efficiency	η_c	0.765
Cruise lift-to-drag ratio	L/D	17
Sea-level air density	ρ	1.225 kg/m^3
Disk loading	δ	450 N/m^2
Battery charge–discharge efficiency	CD	0.9
Primary-to-delivered electricity efficiency	PD	0.408

Appendix B. Sensitivity analysis

The sensitivity analysis focuses on two crucial parameters: eVTOL operating cost per flight and eVTOL power requirement. The two parameters are chosen because of their significant impact on the total operating cost, energy use, and CO_2 emissions in the proposed AAM system. To preserve clarity of the results, the sensitivity analysis is performed based on the first generated instance for each commute route and each eVTOL model. In addition, we vary the demand level and examine how the solution time of the optimization model will change. This examination is useful to understand the scalability of the model.

B.1. eVTOL operating cost

In this appendix, we reduce the variable operating cost per eVTOL flight by 10%, 20%, 30%, 40%, and 50%, to examine how AAM daily operating cost will change. The reductions are applied to both commute routes and both eVTOL models, as shown in Fig. B.13. We can see that using Joby S4, the AAM daily operating cost exhibits greater sensitivity to the per flight variable operating cost than Lilium Jet. The greater sensitivity can be attributed to the larger share of the eVTOL variable operating cost in the daily operating cost for Joby S4 (Fig. 5). In contrast, for Lilium Jet, the eVTOL capital cost holds a significantly larger share in daily operating expenses. Comparing Figs. B.13 and 9, it can be said that when the per flight variable cost is reduced by 50%, the vehicle operating cost for Joby S4 will be reduced by about 35% and become comparable to that of auto commuting by gasoline car on both routes. However, a more significant difference will remain for Lilium Jet.

B.2. eVTOL power requirements

In this appendix, we reduce the eVTOL power requirement across all phases by 10%, 20%, 30%, 40%, and 50%, to examine how daily total energy consumption and CO_2 emissions will change if using AAM to commute. Figs. B.14–B.15 report the results. The energy consumption by auto commuting is also plotted as horizontal lines (black for gasoline car and purple for electric car). On the Northern Cook County-CBD

[4] This assumption of full seat occupancy is actually confirmed in numerical experiments: our results show that the average seat occupancy is above 0.98 for Northern Cook County-CBD commute and above 0.97 for Lake County-CBD commute.

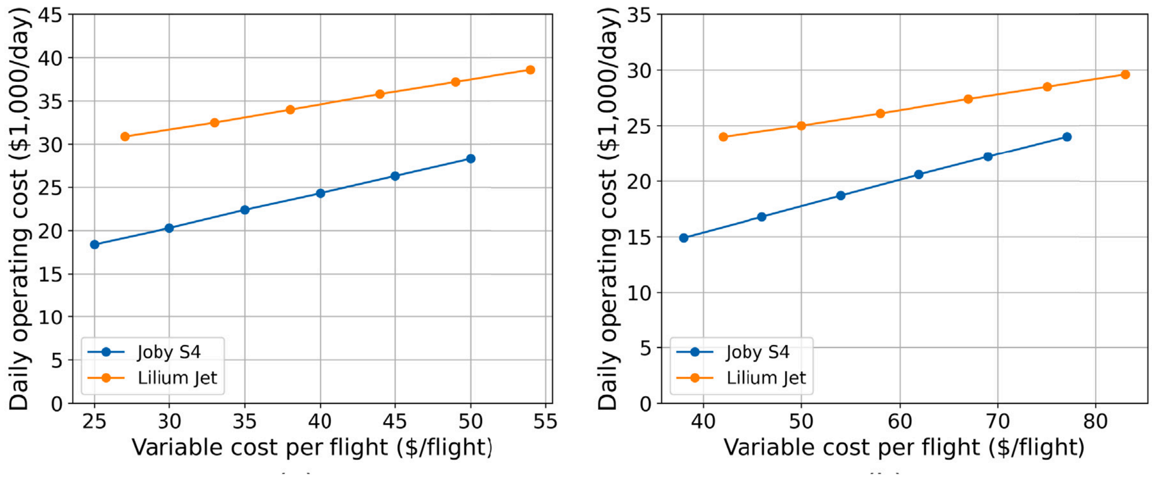

(a) (b)

Fig. B.13. Daily operating cost under different variable cost per flight for Joby S4 and Lilium Jet on (a) Northern Cook County-CBD route and (b) Lake County-CBD route.

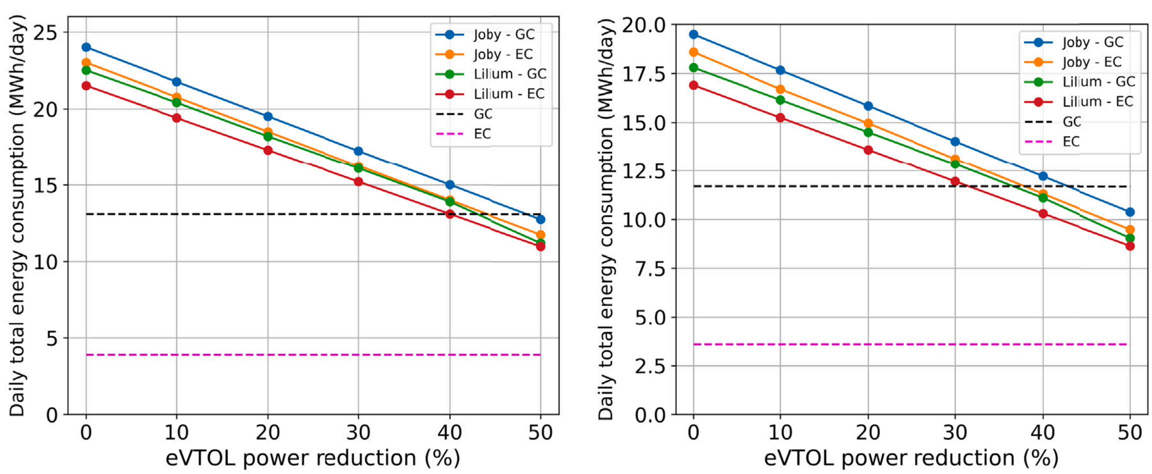

(a) (b)

Fig. B.14. Sensitivity of energy usage to eVTOL power reduction on (a) Northern Cook County-CBD route and (b) Lake County-CBD route (GC: Gasoline car; EC: Electric car).

route, when the eVTOL power requirement is reduced by 50%, the energy use of AAM commuting will fall below that of auto commuting by gasoline car. On the Lake County-CBD route, the extent of reduction will be less for Joby S4 with an electric car for ground access and for Lilium Jet: the energy use of AAM commuting will go below that of auto commuting by gasoline car when the eVTOL power requirement is reduced by 40%. However, the energy use will still be much higher than auto commuting if electric cars are used. The trend is similar for CO_2 emissions, although the extent of reduction is slightly less. For example, when Lilium Jet is used, the eVTOL power requirement only needs to be reduced by 30% in order for the CO_2 emissions to fall below those by gasoline auto commuting. Overall, these percentages indicate that substantial efforts are required to reduce eVTOL power requirements in order to make AAM energy- and emission-competitive with auto for commuting.

B.3. Model solution time under different demand levels

In this appendix, we examine how the solution time of the optimization model will change as we increase the problem size, as reflected in the commuter demand level. For Northern Cook County-CBD, we increase the commuter demand from 357 to 600, 900, 1200, and 1500. For Lake County-CBD, we increase the commuter demand from 199 to 400, 600, 800, and 1000. We assume that the number of takeoff and landing pads at a vertiport (almost) proportionately increases. For example, when demand increases from 357 to 600, the number of takeoff and landing pads at the CBD vertiport is increased from two to four. When the demand further increases to 900, the number of takeoff and landing pads at the CBD vertiport is increased further from four to six. As the number of AAM commuters is increased by up to five times, we are likely to cover and even go above the highest possible AAM commuter demand in early-stage AAM deployment. The generation of commuter home and work locations and time windows follows the same procedure as in Section 4.1.

Fig. B.16 shows the solution time. We can see that the solution time increases almost linearly with the AAM commuter demand, on each commute route and with each eVTOL model. On the Northern Cook County-CBD route, the longest solution time is less than 80 s. On the Lake County-CBD route, the longest solution time is less than 60 s. Given that the long solution time corresponds to very high demand levels and the proposed AAM system is reservation based, solving the optimization model using the SCIP optimization suite seems to be acceptable for eVTOL scheduling.

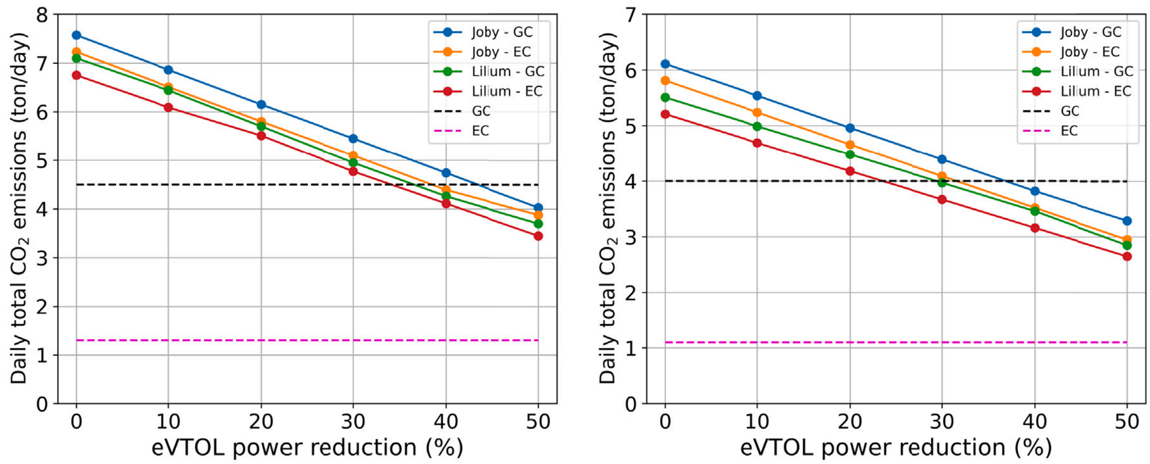

(a) (b)

Fig. B.15. Sensitivity of CO_2 emissions to eVTOL power reduction on (a) Northern Cook County-CBD route and (b) Lake County-CBD route (GC: gasoline car; EC: electric car).

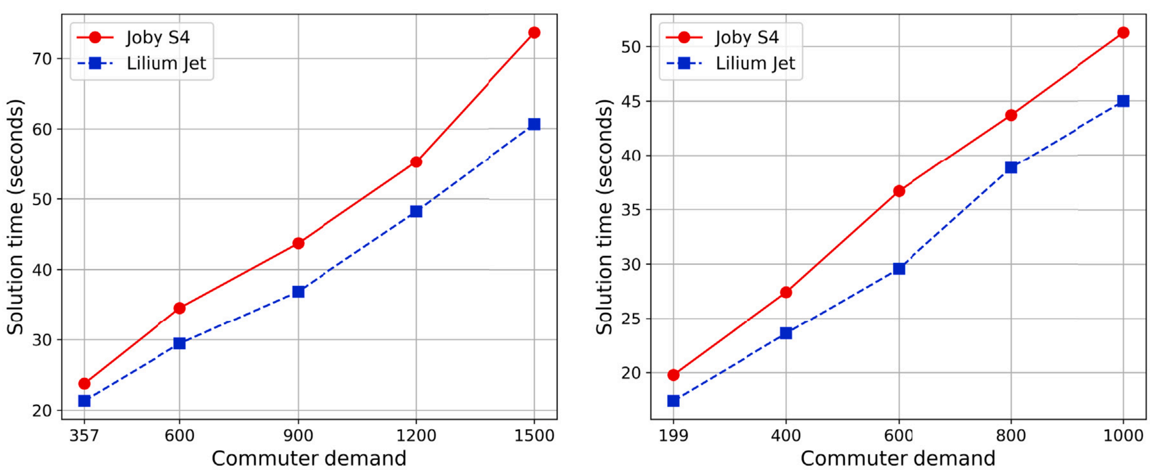

(a) (b)

Fig. B.16. Solution times with different commuter demand: (a) Northern Cook County-CBD and (b) Lake County-CBD.

Data availability

Data will be made available on request.

References

[1] INRIX, INRIX global traffic scorecard, 2025, URL https://inrix.com/scorecard/. (Accessed 18 January 2025).

[2] J.C. Falcocchio, H.S. Levinson, J.C. Falcocchio, H.S. Levinson, The costs and other consequences of traffic congestion, in: Road Traffic Congestion: A Concise Guide, Springer, 2015, pp. 159–182.

[3] T. Afrin, N. Yodo, A survey of road traffic congestion measures towards a sustainable and resilient transportation system, Sustainability 12 (11) (2020) 4660.

[4] Uber Elevate, Fast-forwarding to a future of on-demand urban air transportation, 2016, URL https://evtol.news/_media/PDFs/UberElevateWhitePaperOct2016.pdf.

[5] A. Brown, W.L. Harris, Vehicle design and optimization model for urban air mobility, J. Aircr. 57 (6) (2020) 1003–1013.

[6] Y. Liu, C. Gao, Assessing electric vertical take-off and landing for urban air taxi services: Key parameters and future transportation impact, Sustainability 16 (11) (2024) 4732.

[7] S.A.M. Shihab, P. Wei, D.S.J. Ramirez, R. Mesa-Arango, C. Bloebaum, By schedule or on demand?-a hybrid operation concept for urban air mobility, in: AIAA Aviation 2019 Forum, 2019, p. 3522.

[8] H. Ale-Ahmad, H.S. Mahmassani, Capacitated location-allocation-routing problem with time windows for on-demand urban air taxi operation, Transp. Res. Rec. 2675 (10) (2021) 1092–1114.

[9] N.P. Farazi, B. Zou, Planning electric vertical takeoff and landing aircraft (eVTOL)-based package delivery with community noise impact considerations, Transp. Res. Part E: Logist. Transp. Rev. 189 (2024) 103661.

[10] H. Shon, J. Lee, An optimization framework for urban air mobility (UAM) planning and operations, J. Air Transp. Manag. 124 (2025) 102720.

[11] K. Wang, A. Jacquillat, V. Vaze, Vertiport planning for urban aerial mobility: An adaptive discretization approach, Manuf. Serv. Oper. Manag. 24 (6) (2022) 3215–3235.

[12] L. Chen, S. Wandelt, W. Dai, X. Sun, Scalable vertiport hub location selection for air taxi operations in a metropolitan region, INFORMS J. Comput. 34 (2) (2022) 834–856.

[13] D. Lv, W. Zhang, K. Wang, H. Hao, Y. Yang, Urban aerial mobility for airport shuttle service, Transp. Res. Part A: Policy Pr. 188 (2024) 104202.

[14] S. Rajendran, J. Zack, Insights on strategic air taxi network infrastructure locations using an iterative constrained clustering approach, Transp. Res. Part E: Logist. Transp. Rev. 128 (2019) 470–505.

[15] L.C. Willey, J.L. Salmon, A method for urban air mobility network design using hub location and subgraph isomorphism, Transp. Res. Part C: Emerg. Technol. 125 (2021) 102997.

[16] S. Rath, J.Y. Chow, Air taxi skyport location problem with single-allocation choice-constrained elastic demand for airport access, J. Air Transp. Manag. 105 (2022) 102294.
[17] Z. Jin, K.K. Ng, C. Zhang, Robust optimisation for vertiport location problem considering travel mode choice behaviour in urban air mobility systems, J. the Air Transp. Res. Soc. 2 (2024) 100006.
[18] A. Straubinger, R. Rothfeld, M. Shamiyeh, K.-D. Büchter, J. Kaiser, K.O. Plötner, An overview of current research and developments in urban air mobility–Setting the scene for UAM introduction, J. Air Transp. Manag. 87 (2020) 101852.
[19] E. Lim, H. Hwang, The selection of vertiport location for on-demand mobility and its application to Seoul metro area, Int. J. Aeronaut. Space Sci. 20 (2019) 260–272.
[20] H. Shon, S. Kim, J. Lee, Optimal planning of urban air mobility systems accounting for ground access trips, Int. J. Sustain. Transp. 18 (4) (2024) 356–378.
[21] D. Perez, B. Zou, N.P. Farazi, Package delivery by electric vertical takeoff and landing aircraft? An attractiveness assessment, J. Air Transp. Manag. 124 (2025) 102731.
[22] B. Ahn, H.-Y. Hwang, Design criteria and accommodating capacity analysis of vertiports for urban air mobility and its application at Gimpo Airport in Korea, Appl. Sci. 12 (12) (2022) 6077.
[23] Business Aviation, Vertiports vs. Heliports: A closer look at vertical take-off and landing (VTOL) aircraft gateways, 2024, URL https://businessaviation.aero/evtol-news-and-electric-aircraft-news/advanced-air-mobility/vertiports-vs-heliports-revolutionizing-urban-air-mobility.
[24] P. Brinkmann, Lilium is confident enough in its choice of battery tech to start production of certification aircraft, Aerosp. Am. (2023) URL https://aerospaceamerica.aiaa.org/lilium-is-confident-enough-in-its-choice-of-battery-tech-to-start/-production-of-certification-aircraft/.
[25] Illinois Department of Employment Security, Commuting patterns, 2020, URL https://ides.illinois.gov/resources/labor-market-information/commuting-patterns.html.
[26] US Census, Longitudinal employer-household dynamics, 2021, URL https://lehd.ces.census.gov/data/.
[27] US Census, US census, 2022, URL https://data.census.gov/table?g=040XX00US17.
[28] M. Rimjha, S. Hotle, A. Trani, N. Hinze, Commuter demand estimation and feasibility assessment for urban air mobility in Northern California, Transp. Res. Part A: Policy Pr. 148 (2021) 506–524.
[29] S.-S. Boddupalli, L.A. Garrow, B.J. German, J.P. Newman, Mode choice modeling for an electric vertical takeoff and landing (eVTOL) air taxi commuting service, Transp. Res. Part A: Policy Pr. 181 (2024) 104000.
[30] K.O. Ploetner, C. Al Haddad, C. Antoniou, F. Frank, M. Fu, S. Kabel, C. Llorca, R. Moeckel, A. Moreno, A. Pukhova, et al., Long-term application potential of urban air mobility complementing public transport: an upper bavaria example, CEAS Aeronaut. J. 11 (2020) 991–1007.
[31] CMAP, Travel trends: Understanding how our region moves, 2016, URL https://cmap.illinois.gov/wp-content/uploads/FY17-0012-Travel-Trends-Snapshot.pdf.
[32] Vertical Flight Society, Lilium Jet (seven seater), 2019, URL https://evtol.news/lilium-gmbh-lilium-jet-7-seater.
[33] Vertical Flight Society, Joby aviation S4, 2020, Vertical Flight Society URL https://evtol.news/joby-s4.
[34] R.J. Howard, E. Wright, S.V. Mudumba, N.I. Gunady, B.E. Sells, A. Maheshwari, Assessing the suitability of urban air mobility vehicles for a specific aerodrome network, in: AIAA Aviation 2021 Forum, 2021, p. 3208.
[35] Aviation Base, Inside the 10 million lilium jet, 2023, Aviation Base URL https://www.youtube.com/watch?v=gL1y9p6gEv8&ab_channel=AviationBase.
[36] J. Zhang, Y. Liu, Y. Zheng, Overall eVTOL aircraft design for urban air mobility, Green Energy Intell. Transp. 3 (2) (2024) 100150.
[37] A. Kasliwal, N.J. Furbush, J.H. Gawron, J.R. McBride, T.J. Wallington, R.D. De Kleine, H.C. Kim, G.A. Keoleian, Role of flying cars in sustainable mobility, Nat. Commun. 10 (1) (2019) 1555.
[38] EIA, Illinois state energy profile, Energy Inf. Adm. (2023) URL https://www.eia.gov/state/print.php?sid=IL/.
[39] American Automobile Association, Ownership costs for toyota corolla, 2023, URL https://www.aaa.com/autorepair/drivingcosts/IL-N-2023/Toyota/Corolla/SE%204D%20Sedan%20at/at-15000-miles/on-1-city/fuel-4061.
[40] American Automobile Association, Ownership costs for Tesla model 3, 2023, URL https://www.aaa.com/autorepair/drivingcosts/IL-U-2021/Tesla/Model%203/Standard%20Range%20Plus%204D%20Sedan%20RWD/at-15000-miles/on-1-city/efuel-104.
[41] US Department of Energy, Alternative fuels data center, 2023, URL https://afdc.energy.gov/calc/.
[42] US Department of Energy, Fuel economy, 2021, URL https://www.fueleconomy.gov/feg/topten.jsp.
[43] US Department of Energy, Alternative fuels data center, 2023, URL https://afdc.energy.gov/calc/.
[44] US Department of Energy, Gasoline to co2., 2023, URL https://www.fueleconomy.gov/feg/label/calculations-information.shtml.
[45] US Department of Energy, Greet model, 2023, URL https://www.fueleconomy.gov/feg/topten.jsp.
[46] T. Johnston, R. Riedel, S. Sahdev, To Take Off, Flying Vehicles First Need Places to Land, McKinsey Center for Future Mobility, 2020, pp. 2–8.